Neuromuscular electrical stimulation training induces atypical adaptations of the human skeletal muscle phenotype: a functional and proteomic analysis

Julien Gondin, Lorenza Brocca, Elena Bellinzona, Giuseppe D'Antona, Nicola A. Maffiuletti, Danilo Miotti, Maria A. Pellegrino and Roberto Bottinelli

J Appl Physiol 110:433-450, 2011. First published 2 December 2010;
doi:10.1152/japplphysiol.00914.2010

J Appl Physiol 110: 433–450, 2011.
First published December 2, 2010; doi:10.1152/japplphysiol.00914.2010.

Neuromuscular electrical stimulation training induces atypical adaptations of the human skeletal muscle phenotype: a functional and proteomic analysis

Julien Gondin,[1,2]* Lorenza Brocca,[2]* Elena Bellinzona,[2] Giuseppe D'Antona,[2] Nicola A. Maffiuletti,[4] Danilo Miotti,[3] Maria A. Pellegrino,[2] and Roberto Bottinelli[2]

[1]*Institut National de la Santé et de la Recherche Médicale, U887, Motricité-Plasticité, UFR STAPS, Université de Bourgogne, Campus Universitaire, Dijon, France;* [2]*Department of Physiology and Interuniversity Institute of Myology, University of Pavia, Pavia;* [3]*Fondazione Salvatore Maugeri (IRCCS), Scientific Institute of Pavia, Pavia, Italy;* [4]*Neuromuscular Research Laboratory, Schulthess Clinic, Zurich, Switzerland*

Submitted 9 August 2010; accepted in final form 1 December 2010

Gondin J, Brocca L, Bellinzona E, D'Antona G, Maffiuletti NA, Miotti D, Pellegrino MA, Bottinelli R. Neuromuscular electrical stimulation training induces atypical adaptations of the human skeletal muscle phenotype: a functional and proteomic analysis. *J Appl Physiol* 110: 433–450, 2011. First published December 2, 2010; doi:10.1152/japplphysiol.00914.2010.—The aim of the present study was to define the chronic effects of neuromuscular electrical stimulation (NMES) on the neuromuscular properties of human skeletal muscle. Eight young healthy male subjects were subjected to 25 sessions of isometric NMES of the quadriceps muscle over an 8-wk period. Needle biopsies were taken from the vastus lateralis muscle before and after training. The training status, myosin heavy chain (MHC) isoform distribution, and global protein pattern, as assessed by proteomic analysis, widely varied among subjects at baseline and prompted the identification of two subgroups: an "active" (ACT) group, which performed regular exercise and had a slower MHC profile, and a sedentary (SED) group, which did not perform any exercise and had a faster MHC profile. Maximum voluntary force and neural activation significantly increased after NMES in both groups (+~30% and +~10%, respectively). Both type 1 and 2 fibers showed significant muscle hypertrophy. After NMES, both groups showed a significant shift from MHC-2X toward MHC-2A and MHC-1, i.e., a fast-to-slow transition. Proteomic maps showing ~500 spots were obtained before and after training in both groups. Differentially expressed proteins were identified and grouped into functional categories. The most relevant changes regarded *1*) myofibrillar proteins, whose changes were consistent with a fast-to-slow phenotype shift and with a strengthening of the cytoskeleton; *2*) energy production systems, whose changes indicated a glycolytic-to-oxidative shift in the metabolic profile; and *3*) antioxidant defense systems, whose changes indicated an enhancement of intracellular defenses against reactive oxygen species. The adaptations in the protein pattern of the ACT and SED groups were different but were, in both groups, typical of both resistance (i.e., strength gains and hypertrophy) and endurance (i.e., a fast-to-slow shift in MHC and metabolic profile) training. These training-induced adaptations can be ascribed to the peculiar motor unit recruitment pattern associated with NMES.

exercise training; hypertrophy; motor unit recruitment; two-dimensional electrophoresis; energy metabolism; antioxidant defense

OVER THE LAST 30 YR, numerous studies have characterized in vivo the effects of multiple sessions of neuromuscular electrical stimulation (NMES) on skeletal muscle function. In both healthy and impaired muscles, it has been commonly reported that NMES is an efficient modality for increasing muscle mass (36, 82), maximal voluntary strength (36, 82), and/or exercise capacity (16, 72). On that basis, NMES has been widely used as a complement to voluntary exercise in athletes (64) and in patients who cannot undertake conventional forms of voluntary exercise due various pathologies such as heart failure (82), chronic obstructive pulmonary disease (72), or cancer (22).

Although growing evidence is emerging illustrating the beneficial effects of NMES training programs in humans, the corresponding cellular and molecular mechanisms responsible for the improved muscle function remain very poorly documented, whereas a plethora of studies have described those occurring after voluntary resistance training (for reviews, see Refs. 20 and 94). Indeed, muscle biopsy samples have been scarcely analyzed in response to multiple bouts of NMES, and most of the previous human studies (33, 74, 92, 93) have been focused on the chronic effects of low-frequency NMES. In the corresponding experiments, both the stimulation frequency (from 8 to 15 Hz) and amounts of daily stimulation (from 3 to 8 h) were far from those commonly used in sport training and rehabilitation programs (i.e., ~50–75 Hz for ~15–30 min, respectively) (60). To our knowledge, only two studies have performed in vitro analyses after conventional NMES resistance training. Perez et al. (77) demonstrated a shift toward a slower phenotype after a 6-wk NMES program (3 days/wk with a 45- to 60-Hz intermittent pattern). Surprisingly, these authors failed to observe muscle hypertrophy and an improvement in functional capacity of the knee extensor muscles. Although a single case study (65) has combined both in vivo and in vitro experiments and reported important clues to changes in maximal voluntary strength, neural activation, myosin heavy chain (MHC) composition, and single fiber morphology, such investigations need to be extended to a larger sample size. This is of the utmost interest as adaptations to NMES could differ from those observed after voluntary training. Indeed, NMES is characterized by a nonselective, spatially fixed (i.e., continuous), and temporally synchronous motor unit recruitment pattern (37), while it is well acknowledged that motor units are recruited according to the size principle during voluntary contractions (42). As a consequence, NMES may recruit both slow and fast fibers even at relatively low force levels (i.e., random spatial recruitment) (53). In addition, NMES would lead to a continuous activation of the same muscle fibers, thereby resulting in an exaggerated metabolic demand and muscle fatigue (for a review, see Ref. 63). Considering this peculiar motor unit recruitment, NMES could induce adaptations of the muscle phenotype different from and

* J. Gondin and L. Brocca contributed equally to this work.

Address for reprint requests and other correspondence: R. Bottinelli, Dept. of Physiology and Interuniversity, Institute of Myology, Univ. of Pavia, Via Forlanini 6, 27100 Pavia, Italy (e-mail: roberto.bottinelli@unipv.it).

complementary to those obtained with voluntary training, which might be particularly suited to treat specific conditions of disuse/immobilization. NMES could also offer significant advantages over voluntary training as it could be applied to subjects with limited or no compliance to volitional exercise, such as elderly and very sedentary subjects, patients affected by cardiac and respiratory chronic diseases, and patients in intensive care units, who can undergo critical illness myopathy characterized by extensive muscle atrophy.

The present study aimed to provide a comprehensive picture of skeletal muscle phenotype adaptations after a typical NMES training program known to induce voluntary strength gains (36). Maximal voluntary strength and neural activation (assessed by the twitch interpolation technique) were used to characterize in vivo the chronic effects of NMES on the neuromuscular properties of the knee extensor muscles. Needle biopsy samples were taken from the vastus lateralis muscle before and immediately after the training period and used for an analysis of MHC isoform distribution and for proteome analysis. Since almost 20 yr, MHC isoform distribution has emerged as the major single marker of muscle phenotype adaptations (13, 25, 41) based on the key functional role of myosin isoforms and on the understanding that a gene expression program coordinates the expression of MHC isoforms and many other myofibrillar and nonmyofibrillar proteins (13, 86). Much more recently, it has been suggested that skeletal muscle adaptations would not depend on a single "master switch" shifting MHC isoforms and the muscle phenotype from slow to fast or vice versa (88). On the contrary, a number of broad genetic programs can control the expression of proteins belonging to different functional categories, generating adaptations in the protein pattern, which are much more complex than a shift in MHC distribution and in the related proteins. To address the complexity of the phenomenon, proteomic analysis appeared to be the approach of choice. Proteomic analysis, in fact, has been shown to provide a global analysis of the adaptations in the protein pattern of a muscle identifying the differentially expressed proteins, which can be considered the target of an adaptive phenomenon, among a very large number of proteins (500–800) (17, 18, 34).

Combining functional analyses in vivo with proteomic analysis in vitro, this study suggests that NMES, likely due to specific motor unit recruitment, causes atypical adaptations of the muscle phenotype that appear particularly suited to counteract disuse atrophy. This study is the first of a series of NMES training investigations in which it is essential to understand the chronic response of healthy muscles before studying what happens to immobilized/disused muscles.

METHODS

Experimental Design

This study was performed on 10 healthy young men (age: 26 ± 3 yr, height: 177 ± 8 cm, and weight: 75 ± 13 kg) with no previous record of muscular disease or traumatic lesions who volunteered to participate in the investigation. None of them had engaged in systematic strength training or NMES in the 12 mo before the beginning of the experiments. However, five subjects were involved in various sports (basketball, kickboxing, track and field, and mountain climbing) and were mainly recruited from the Faculty of Sport Sciences of the University of Pavia. The average weekly volume of physical exercise was ~4–6 h/wk. The five remaining subjects, who were mainly recruited from the Medical School of the University of Pavia, had no history of regular participation in physical activities (i.e., <2 h/wk). The study was approved by the ethical committee of the University of Pavia and conformed with standards set by the Declaration of Helsinki (last modified in 2000). The quadriceps femoris muscles of both legs were trained for 8 wk. Neuromuscular tests were performed 4 days before the first training session and 4 days after the last training session. Biopsy samples were obtained from the right vastus lateralis muscle for 9 subjects and from the left vastus lateralis muscle for 1 subject at least 2 wk before the beginning of the NMES training program and immediately after the last NMES training session. One subject dropped out due to personal problems, and another subject was excluded from the data analysis due to a specific MHC distribution (see below). Therefore, both in vivo and in vitro results were obtained from eight subjects.

NMES Training

The training program consisted of 25 18-min sessions of isometric (bilateral) NMES over an 8-wk period, with 3 sessions/wk. Each training session was composed of 40 isometric contractions. During the stimulation, subjects were seated on a leg extension machine (Oemmebi, Moglia, Italy) typically used for strength training of the quadriceps muscle with the knee joint fixed at a 75° angle (where 0° corresponds to a full knee extension). Straps were firmly fastened across the pelvis to minimize hip and thigh motion during the contractions. Three 2-mm-thick, self-adhesive electrodes were placed over each thigh. Two positive electrodes, measuring 25 cm^2 (5 × 5 cm), were placed as close as possible to the motor point of the vastus lateralis and vastus medialis muscles. The negative electrode, measuring 50 cm^2 (10 × 5 cm), was placed 5–7 cm below the inguinal crease. For each individual, the set of the electrodes was changed at the end of the fourth week of training. A portable battery-powered stimulator (Compex Sport, Medicompex, Ecublens, Switzerland) was used. Rectangular wave pulsed currents (75 Hz) lasting 400 μs were delivered with a rise time of 1.5 s, a steady tetanic stimulation time of 4 s, and a fall time of 0.75 s (total duration of the contraction: 6.25 s). Each stimulation was followed by a pause lasting 20 s. Intensity was monitored online and was gradually increased throughout the training session to a level of maximally tolerated intensity. Each session was preceded by a standardized warmup consisting of 5 min of submaximal electrical stimulation at a freely chosen intensity (5 Hz, pulses lasting 200 μs). Subjects then performed two maximal isometric voluntary contractions (MVCs) of the knee extensor muscles separated by 2 min of rest. The individual level of isometric force developed during each NMES session was measured using a strain gauge (load cell model DG-ST, Dinamica Generale, Poggio Rusco, Italy). The peak force of each evoked contraction was measured and then divided by the highest MVC obtained before the NMES training session. Such a NMES training protocol has been successfully used in our laboratory to increase knee extensor muscle strength (36).

As described in detail below, subjects were separated in two groups: an active (ACT) group and a sedentary (SED) group. The average force evoked during the NMES session was not different ($P > 0.05$) between the two groups (56 ± 8% vs. 59 ± 5% MVC for the ACT and SED groups, respectively). In the same way, stimulation intensity was similar ($P > 0.05$) between the groups despite large inter- and intragroup variability (81 ± 27 vs. 61 ± 20 mA for the ACT and SED groups, respectively).

In Vivo Neuromuscular Tests

The testing session included MVCs of the knee extensor muscles with neural activation assessment (see below). All measurements were carried out on the biopsied leg. The present experimental protocol and procedures are commonly adopted in our laboratory for the study of neuromuscular properties of the knee extensor muscles (36). All contractions were performed under isometric conditions using an

isometric ergometer that included a chair connected to a strain gauge (see above). Subjects were placed in a seated posture with the trunk-thigh angle at 90° and the knee flexed at 75°, as in the NMES training position. Each subject was securely strapped to the test chair with two crossover shoulder harnesses and a belt across the hip joint. A strap also secured the lower leg of the subject to the ergometer lever arm.

Before each testing session, 10–15 submaximal voluntary contractions were completed before the determination of the optimal intensity for electrically evoked twitch and doublet. The femoral nerve was stimulated using a cathode ball electrode (0.5-cm diameter) manually pressed and maintained in the femoral triangle 3–5 cm below the inguinal ligament. The anode was a large electrode (10 × 5 cm) located in the gluteal fold. Rectangular pulses (1-ms duration, 400-V maximal voltage) were delivered by a commercially available stimulation unit (Digitimer DS7, Hertfordshire, UK). Stimulation intensity was progressively increased by 10-mA increments until there was no further increase in peak twitch force (i.e., the highest value of the quadriceps twitch force). This intensity was further increased by 10% (i.e., supramaximal) and then maintained for paired stimulations (10-ms interpulse interval).

MVC force of the knee extensor muscles (2–3 trials) muscle was measured, during which subjects were instructed to produce their maximal force ("hard"). The total duration of these efforts was ~5 s. Paired stimuli were delivered over the isometric plateau (superimposed doublet) and 8 s after the contractions (potentiated doublet) to assess neural activation according to the twitch interpolation technique (4). A 2-min rest period was allowed between MVCs to minimize the effects of fatigue.

Force traces were digitized online (sampling frequency: 5 kHz) and stored for analysis with commercially available software (Acknowledge, Biopac Systems, Santa Barbara, CA). MVC force was analyzed over a 500-ms period once the isometric force had reached a plateau and before the superimposed stimuli. Neural activation was estimated according to the following formula: (1 − superimposed doublet/potentiated doublet) × 100 (4). Only the trial with the highest MVC force was considered for analysis.

In Vitro Analyses

Muscle samples (~50–100 mg) were taken from the vastus lateralis muscle by needle biopsy under local anaesthesia using the Bergstrom approach, which is routinely used in our laboratory (12, 24, 25). Biopsies were divided in two portions of different size: the larger one was immediately frozen in liquid nitrogen and thereafter used for MHC and proteomic analysis and the smaller one was mounted in an embedding medium (Tissue-Tek) and frozen in liquid nitrogen.

MHC isoform analysis. Separation and identification of MHC isoforms were performed according to our previous reports (24, 25). MHC distribution was initially obtained in nine subjects. MHC distribution widely varied among subjects and prompted the identification of two subgroups. K-means cluster analysis has recently emerged as a relevant tool for classifying human subjects based on the magnitude of myofiber hypertrophy in response to voluntary resistance training protocols (9, 58, 78, 79). This kind of analysis is of interest for investigating the highly variable nature of training-mediated adaptations between human subjects. Using K-means statistical analysis, we classified subjects into two groups (or clusters) based on their MHC distribution: subjects having a MHC-2X content of <9% and MHC-1 of >23% and subjects having a MHC-2X content of >34% and MHC-1 of <12%. It is noteworthy that one subject had an atypical MHC isoform distribution (MHC-1: 21%, MHC-2A: 38%, and MHC-2X: 41%) and was not included in the cluster analysis. Therefore, each group analyzed for MHC, and the proteomic was composed of four subjects. Interestingly, all subjects of the first group (low MHC-2X content) were students from the Faculty of Sport Sciences of the University of Pavia who were more active, whereas all subjects of the second group (high MHC-2X content) were students from the Faculty of Medicine of the University of Pavia who were less active. Consequently, the subgroup with low MHC-2X content was called the ACT group (age: 25 ± 3 yr, height: 175 ± 6 cm, and weight: 75 ± 14 kg), whereas the group with high MHC-2X content was called the SED group (age: 26 ± 4 yr, height: 175 ± 8 cm, and weight: 71 ± 12 kg).

Cross-sectional area analysis. The cross-sectional area (CSA) of individual muscle fibers was determined in four subjects. Although a portion of each biopsy was embedded and frozen in liquid nitrogen for such analysis, the size of the bundle enabled a precise determination of the CSA of muscle fibers in only four subjects. Most of the biopsy was, in fact, used for MHC and proteomic analysis, which were the major goals of the study. Serial transverse sections (10 μm thick) of the muscle samples mounted in OCT embedding medium were cut in a cryostat at −20°C. The cross-cryosections were incubated for 40 min with primary antibody against MHC isoforms (BA-F8 against MHC-1 and SC-71 against MHC-2A) as previously described in detail (14); after several washes in PBS (136 mM NaCl, 2 mM KCl, 6 mM Na_2KPO_4, and 1 mM KH_2PO_4), the cross-cryosections were incubated with secondary antibody (rabbit anti-mouse IgG) conjugated with peroxidase (DAKO P-0260) to reveal the binding of the primary antibodies. The antibodies enabled us to identify type 1 and type 2A muscle fibers. As no antibodies are available against MHC-2X, analysis could not be performed on such fibers. Images of the stained sections were captured using a light microscope (Leica DMLS) and transferred to a personal computer using a video camera (Leica DFC 280). CSAs of identified fibers were measured with Scion Image analysis software (National Institutes of Health, Bethesda, MD) and expressed in micrometers squared. Approximately 200 fibers/muscle were measured.

Proteome Analysis (Two-Dimensional Electrophoresis)

Sample preparation. The methods of proteome analysis were mostly the same as those previously used (17). Muscle samples previously stored at −80°C were pulverized in a steel mortar with liquid nitrogen to obtain a powder that was immediately resuspended in lysis buffer (8 M urea, 2 M thiourea, 4% CHAPS, 65 mM DTT, and 40 mM Tris base; 10 μl buffer/mg tissue). Samples were vortexed, frozen with liquid nitrogen, thawed at room temperature four times, incubated with DNase and RNase for 45 min at 4°C to separate proteins from nucleic acids, and then spun at 35,000 *g* for 30 min. The protein concentration in the dissolved samples was determined with a protein assay kit [two-dimensional (2-D) quant kit, GE Healthcare].

To perform proteome analysis, a sample mix was created for each experimental group (ACT and SED) both pre- and post-NMES training. Each sample mix was constituted by an equal protein quantity from each subject. Isoelectrofocusing was carried out using an IPGphor system (Ettan IPGphor Isoelectric Focusing Sistem, Amersham Biosciences). IPG gel strips [pH 3–11 nonlinear (NL), 13 cm] were rehydrated for 14 h at 30 V and 20°C in 250 μl of reswelling buffer [8 M urea, 2 M thiourea, 2% (wt/vol) CHAPS, 0.1% (vol/vol) tergitol NP7 (Sigma), 65 mM DTT, and 0.5% (vol/vol) pharmalyte 3–11 NL (Amersham Biosciences)] containing 100 μg of protein sample. Strips were focused at 20,000 V·h at a constant temperature of 20°C, and the current was limited to 50 μA/IPG gel strip. After isoelectrofocusing, the strips were stored at −80°C until use or equilibrated immediately for 10–12 min in 5 ml of equilibration buffer [50 mM Tris (pH 6.8), 6 M urea, 30% (vol/vol) glycerol, 2% (wt/vol) SDS, and 3% (wt/vol) iodoacetamide]. The immobiline IPG gel strips were then applied to 15% T and 2.5% C polyacrilamide gels without a stacking gel. The separation was performed at 80 V for 17 h at room temperature.

The 2-D gels were fixed for 2 h in fixing solution [40% (vol/vol) ethanol and 10% (vol/vol) acetic acid], stained with fluorescent staining (FlamingoTM Fluorescent Gel Stain, Bio-Rad) for 3 h, and destained with 0.1% (wt/vol) Tween 20 solution for 10 min. Triplicate

gels of each sample were acquired by a Typhoon system. Image analysis was carried out using Platinum Software (GE Healthcare), which provided the normalized volume for each spot (representing the amount of protein). The volumes of each spot in the triplicate gels were averaged. The average volumes (±SD) were used for statistical comparison among spots that were considered differentially expressed if $P < 0.05$ by a *t*-test. The average volumes of each differentially expressed spot were also used to determine the volume ratios reported in the figures.

Protein identification. ELECTROPHORESIS FRACTIONATION AND IN SITU DIGESTION. For protein identification, 2-D gels were loaded with 300 μg proteins/strip; the electrophoretic conditions were the same as those described above. After being stained with colloidal Comassie, spots were excised from the gel and washed in 50 mM ammonium bicarbonate (pH 8.0) in 50% acetonitrile to a complete destaining. The gel pieces were resuspended in 50 mM ammonium bicarbonate (pH 8.0) containing 100 ng trypsin and incubated for 2 h at 4°C and overnight at 37°C. The supernatant containing the resulting peptide mixtures was removed, and the gel pieces were reextracted with acetonitrile. The two fractions were then collected and freeze dried.

MATRIX-ASSISTED LASER DESORPTION/IONIZATION MASS SPECTROSCOPY ANALYSIS. Matrix-assisted laser desorption/ionization (MALDI) mass spectra were recorded on an Applied Biosystem Voyager DE-PRO mass spectrometer equipped with a reflectron analyzer and used in the delayed extraction mode. One microliter of peptide sample was mixed with an equal volume of α-cyano-4-hydroxycynnamic acid as matrix [10 mg/ml in 0.2% trifluoroacetic acid (TFA) in 70% acetonitrile], applied to the metallic sample plate, and air dried. Mass calibration was performed using the standard mixture provided by manufacturer. Mass signals were then used for database searching using the MASCOT peptide fingerprinting search program (Matrix Science, Boston, MA) available online.

LIQUID CHROMATOGRAPHY TANDEM MASS SPECTROSCOPY ANALYSIS. When the identity of the proteins could not be established by peptide mass fingerprinting, the peptide mixtures were further analyzed by liquid chromatography tandem mass spectroscopy (LCMSMS) using a LC/MSD Trap XCT Ultra (Agilent Technologies, Palo Alto, CA) equipped with a 1100 HPLC system and a chip cube (Agilent Technologies). After being loaded, the peptide mixture (7 μl in 0.5% TFA) was first concentrated and washed *1*) at 1 μl/min onto a C18 reverse-phase precolumn (Waters) or *2*) at 4 μl/min in a 40-nl enrichment column (Agilent Technologies chip) with 0.1% formic acid as the eluent. The sample was then fractionated on a C18 reverse-phase capillary column (75 mm × 20 cm in the Waters system and 75 × 43 mm in the Agilent Technologies chip) at a flow rate of 200 nl/min with a linear gradient of *eluent B* (0.1% formic acid in acetonitrile) in *eluent A* (0.1% formic acid) from 5% to 60% in 50 min. Elution was monitored on the mass spectrometers without any splitting device. Peptide analysis was performed using data-dependent acquisition of one MS scan (*m*/*z* range from 400 to 2,000 Da/electron) followed by MS/MS scans of the three most abundant ions in each MS scan. Dynamic exclusion was used to acquire a more complete survey of the peptides by automatic recognition and temporary exclusion (2 min) of ions from which definitive MS data had previously been acquired. Moreover, a permanent exclusion list of the most frequent peptide contaminants (keratins and trypsin peptides) was included in the acquisition method to focus the analyses on significant data.

Immunoblot Analysis

Protein variations observed with the proteomic approach were also investigated with standard one-dimensional immunoblot analysis to confirm the variation of protein expression.

About 30 μg of muscle samples prepared and used for 2-D electrophoresis were loaded on 15% SDS-PAGE gels. Proteins were transferred from the gels to nitrocellulose membranes (4.5 μm pore size, GE Healthcare), and Western blot analysis was performed. Nitrocellulose membranes were blocked in 5% milk in Tris-buffered saline (TBS; 0.02 M Tris and 0.05 M NaCl, pH 7.4–7.6) for 1 h and then incubated in primary antibody (diluted in 5% milk) at 4°C overnight. The following antibodies were used: ATP synthase-β (rabbit anti-ATP synthase, dilution 1:2,000, Abcam), NADH-ubiquinone oxidoreductase 30-kDa subunit (mouse anti- NADH-ubiquinone oxidoreductase, 1:5,000, Abcam), ubiquinol cytochrome *c* reductase (mouse anti-ubiquinol cytochrome *c* reductase 1, 1:1,000, Abnova), tubulin (rabbit anti-tubulin, 1:300, Abcam), SOD1 (rabbit anti-SOD1, 1:900, Abcam), peroxiredoxin (PRDX)3 (mouse anti-PRDX3, 1:500, Abcam), αβ-crystallin (rabbit anti-αβ-crystallin, 1:1,000, Abcam), acyl CoA (mouse anti-acyl CoA, 1:1,000, Abnova), pyruvate dehydrogenase (mouse anti-pyruvate dehydrogenase, 1:500, Abcam), isocitrate dehydrogenase (rabbit anti-isocitrate dehydrogenase, 1:500, Abcam), lactate dehydrogenase (rabbit anti-lactate dehydrogenase, 1:1,000, Abcam), triosephosphate isomerase (mouse anti-triosephosphate isomerase, 1:1,000, Abcam), β-enolase (mouse anti-β-enolase, 1:1,000, Abnova), creatine kinase M (rabbit anti-creatine kinase M, 1:1,000, Abcam), and myoglobin (rabbit anti-myoglobin, 1:2,000, Abcam).

After several rinses in 0.1% Tween 20 in TBS, membranes were incubated in horseradish peroxidase-conjugated secondary antibody (diluted in 5% milk), rabbit anti-mouse (1:800, DAKO) or goat anti-rabbit (1:5,000, Millipore), for 1 h at room temperature. Protein bands were visualized by an enhanced chemiluminescence method in which luminol was excited by peroxidase in the presence of H_2O_2 (ECL Plus, GE Healthcare). The content of a single protein under investigation was assessed by determining the brightness-area product of the protein bands.

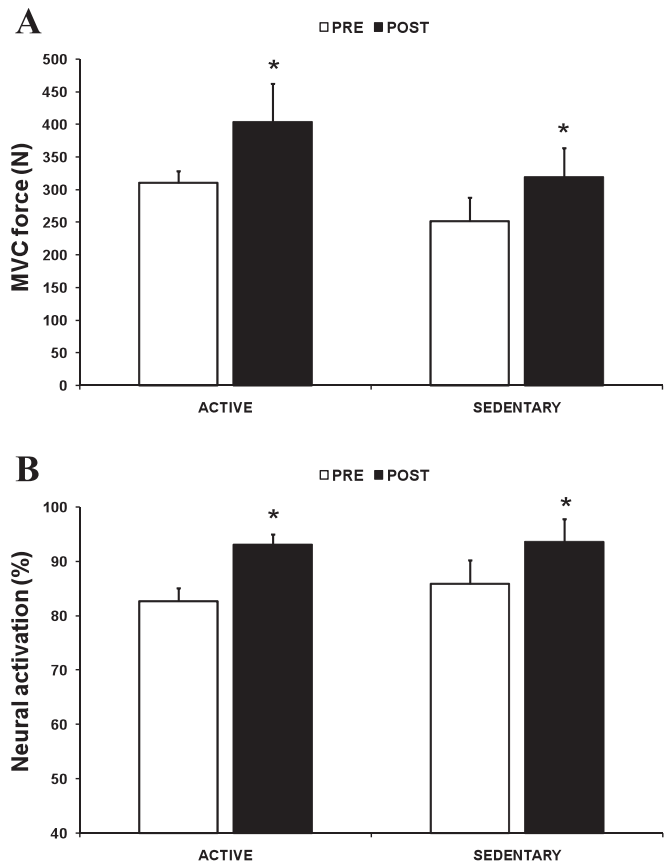

Fig. 1. Maximal voluntary contraction (MVC) force obtained during unilateral knee extension with the biopsied leg (*A*) and neural activation assessed by the twitch interpolation technique (*B*) before (Pre) and after (Post) neuromuscular electrical stimulation (NMES) training for both the active (ACT) and sedentary (SED) groups. *Significantly different from pre-NMES ($P < 0.05$).

Statistical Analysis

K-means statistical analysis was performed to identify two clusters based on the MHC isoform distribution (Statistica 6.0, Statsoft, Tulsa, OK). Statistical significance of the differences between means was assessed by Student's *t*-test. Paired *t*-tests were used for the comparison between pre- and post-NMES data. Unpaired *t*-tests were used to compare the changes between ACT and SED groups. A probability of <5% was considered significant ($P < 0.05$). All data are expressed as means ± SD within the text (few occurrences) and as means ± SE in the figures for the sake of clarity.

RESULTS

MVC Force and Neural Activation

MVC force increased significantly ($P < 0.05$) and similarly for both groups (+29 ± 20% and +27 ± 20% for the ACT and SED groups, respectively) after training (Fig. 1*A*). There was a trend toward a significant higher MVC force ($P = 0.13$) at baseline for the ACT group compared with the SED group. Neural activation was significantly higher ($P < 0.05$) post-NMES for both the ACT (+13 ± 4%) and SED (+9 ± 5%) groups (Fig. 1*B*). Despite the different training background between the two groups, neural activation was not different at baseline, likely due to the small sample size.

CSA of Individual Muscle Fibers

CSA of type 1 and 2A individual muscle fibers was determined on cross-cryosections of muscle bundles stained by monoclonal antibodies against MHC-1 and MHC-2A (Fig. 2*A*). For technical reasons, the analysis could be performed on four subjects only (see METHODS). Therefore, no comparison between the subjects belonging to the ACT ($n = 2$) and SED ($n = 2$) groups was performed, as it would not have had statistical significance, and all data were pooled. Both fiber types went through hypertrophy after NMES training (Fig. 2*B*), which was higher in fast type 2A fibers (+23%) compared with slow type 1 fibers (+12%).

MHC Distribution

As indicated in METHODS, MHC isoform distribution widely varied among subjects and prompted the identification of two subgroups (or clusters): the ACT group and the SED group (Fig. 3). For both groups, MHC isoform distribution shifted toward a slower phenotype after NMES (Fig. 3). In the ACT group, we observed a significant increase in MHC-1 content (+20%) and a concomitant reduction (−9%) in MHC-2A relative content. In the SED group, both the MHC-1 and MHC-2A contents were higher (+96% and +42%, respec-

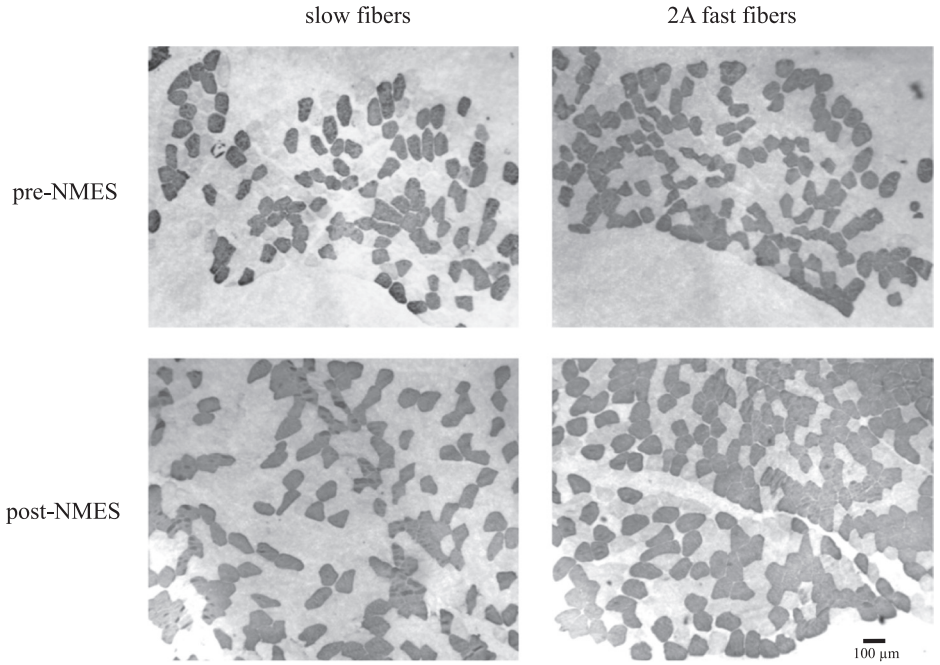

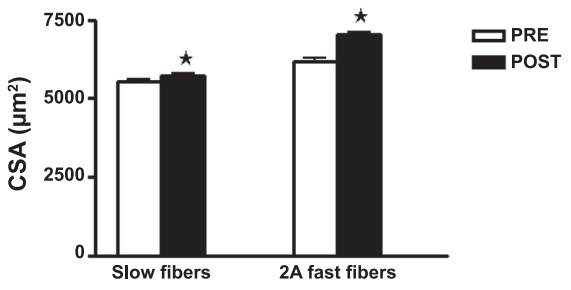

Fig. 2. Cross-sectional area (CSA) determined on cross-cryosections immunostained by an anti-myosin heavy chain (MHC)-1 and anti-MHC-2A antibodies for a representative subject (*A*) and all subjects (*B*) pre- and post-NMES training. Four subjects were analyzed. *Significantly different from pre-NMES ($P < 0.05$).

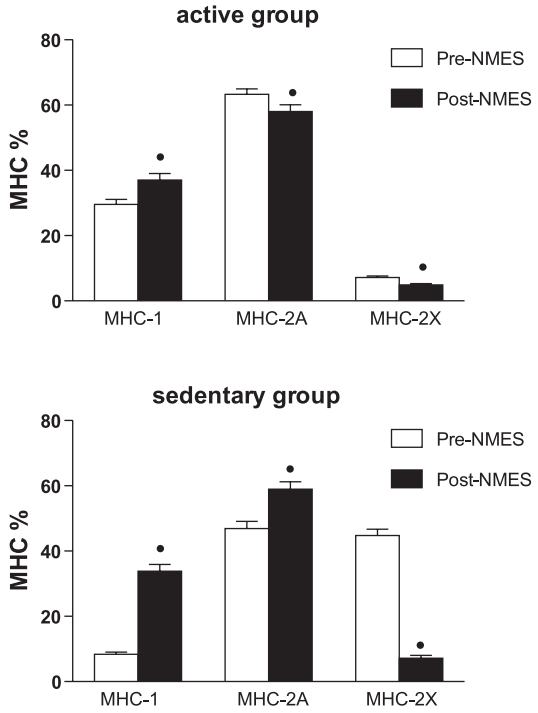

Fig. 3. MHC isoform distribution pre- and post-NMES training for the ACT and SED groups. *Significantly different from pre-NMES ($P < 0.05$).

tively) post-NMES, whereas a large decrease was observed (−79%) in MHC-2X. Interestingly, the MHC profile of the SED group after training was not significantly different from that of the ACT group at baseline. Moreover, the MHC profile of the two groups converged toward a common pattern post-NMES, so that post NMES the two groups were much more similar than at baseline.

Adaptations of the Protein Pattern

2-D maps were obtained, pooling equal amounts of muscle samples from ACT and SED subjects. Although the goal of the work was to study the adaptations in the protein pattern after NMES, as two groups were identified by K-means analysis based on the MHC isoform distribution, the proteomic map of the ACT group pre-NMES was first compared with that of the SED group pre-NMES to define baseline differences in the protein pattern. Thereafter, the major comparisons between the ACT group pre- and post-NMES and between the SED group pre- and post-NMES were performed.

After all comparisons, the differentially expressed proteins were grouped on the basis of their functional role into the following categories: myofibrillar proteins, energy production systems (glycolytic metabolism, oxidative metabolism, and creatine kinase), antioxidant defense systems, and heat shock proteins (HSPs). The remaining proteins, with variable functional roles, were pooled into a single group (other proteins).

The circles and numbers shown in Fig. 4 indicate all proteins found to be differentially expressed in any of the comparisons performed and that could be identified by MALDI-time of flight (MALDI-TOF). The numbers enable the identification of the protein and access to the full set of information regarding the differentially expressed proteins shown in Tables 1–3.

Four hundred and sixty-three protein spots were common to both ACT and SED groups pre-NMES, 52 protein spots were differentially expressed (44 upregulated and 8 downregulated), and 23 protein spots were identified by MALDI-TOF (Fig. 5). The content in glycolytic enzymes and creatine kinase were higher, whereas that of oxidative enzymes was lower in the SED group than in the ACT group. Four myofibrillar protein isoforms were differentially expressed: myosin light chain (MLC)-2s was downregulated, whereas MLC-2f, troponin T fast, and tropomyosin-α fast were upregulated. Carbonic anhydrase III was upregulated in the SED group compared with the ACT group. Fatty acid-binding proteins, serum albumin, myoglobin, and DNAase1 were also upregulated in the SED group compared with the ACT group. The full set of information regarding the differentially expressed proteins is shown in Table 1.

As regards the impact of NMES on the protein pattern of the ACT and SED groups, in the ACT group, 500 protein spots were separated on 2-D gels. Thirty-nine spots (~8%) were differentially expressed after NMES, of which 22 were identified by MALDI-TOF (Fig. 6). In the SED group, 510 spots were separated in proteomic maps. Forty-two spots (~8%) were differentially expressed, of which 31 were identified by MALDI-TOF (Fig. 7). The full set of information regarding the differentially expressed proteins in both groups is shown in Tables 2 and 3.

As frequently observed in 2-D gels, several of the differentially expressed proteins were found at multiple spot locations and therefore appear more than once in the figures and tables. Spots of some MLCs varied in opposite directions and suggested a separate analysis (Fig. 8), whereas all other differentially expressed spots, except pyruvate kinase (Fig. 7), varied in the same direction.

Myofibrillar proteins. Seven and four myofibrillar protein spots were differentially expressed in the ACT and SED groups, respectively. In the ACT group MLC-1s content was higher and in the SED group MLC-2f and troponin T fast content were lower post-NMES. In the SED group, two spots corresponding to MLC-1f were significantly changed: one was upregulated and the other was downregulated. Several other spots corresponding to MLC isoforms were differentially expressed, but their changes did not reach statistical significance. In an attempt to define a more comprehensive picture of MLC isoforms adaptations, we pooled the volumes of all spots of a given MLC isoform and compared their content pre-NMES versus post-NMES in both the ACT and SED groups (Fig. 8). The analysis indicated an overall fast-to-slow shift in MLC isoforms after NMES.

Besides MLCs, in the ACT group, α-cardiac and α-skeletal actin, tubulin (β2-chain, two spots), desmin, and cofilin-2 were significantly upregulated. Interestingly, besides MLCs and troponin T fast, no other myofibrillar proteins were differentially expressed in the SED group.

Energy production systems. In the ACT group, all the differentially expressed proteins involved in glycolytic ($n = 1$) and oxidative metabolism ($n = 4$) were upregulated. Enoyl-CoA hydratase was included in this functional group as it catalyzes the second step in the β-oxidation pathway of fatty acid metabolism.

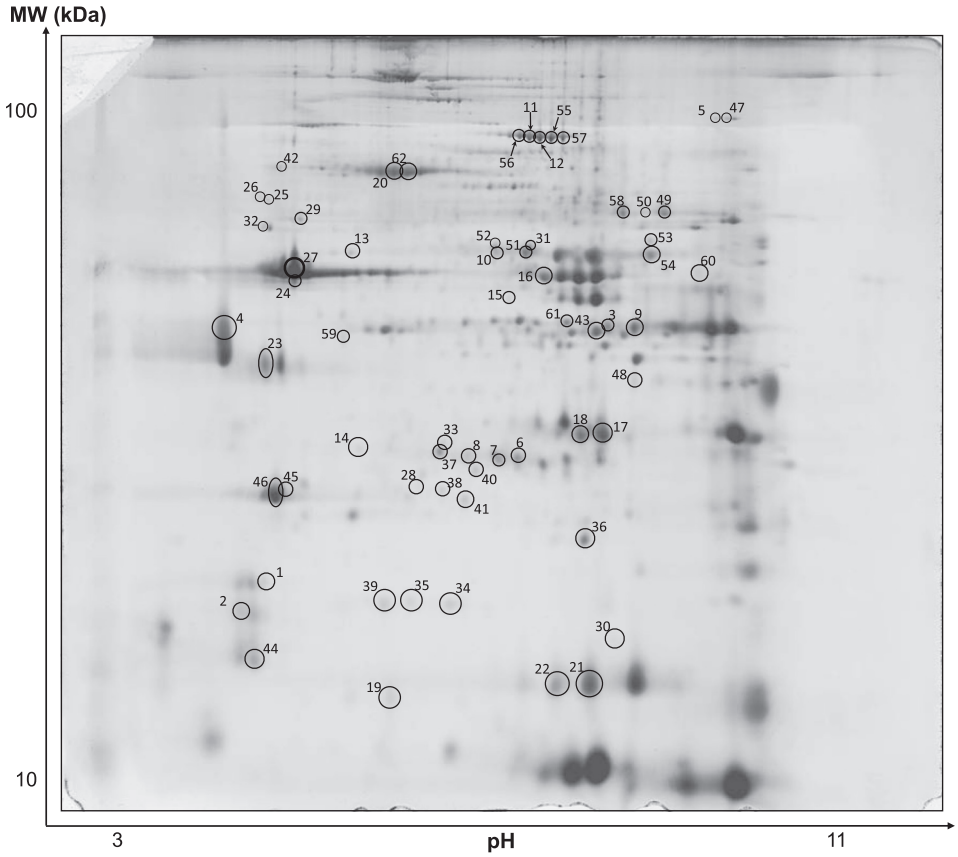

Fig. 4. Representative two-dimensional gel of a vastus lateralis muscle sample (active subject pre-NMES). Thirteen-centimeter IPG gel strips (pH 3–11 nonlinear) were used in the first dimension, and SDS gels (15% T and 2.5% C) were used in the second dimension. The differentially expressed protein spots found in any of the comparisons (ACT group vs. SED group pre-NMES, ACT group pre-NMES vs. ACT group post-NMES, and SED group pre-NMES vs. SED group post-NMES) are circled and numbered. The numbers enable identification of the circled spots using Tables 1–3.

In the SED group, glycolytic enzymes (16 spots, 7 proteins) and creatine kinase were mostly downregulated and oxidative enzymes ($n = 4$) were mainly upregulated

Antioxidant defense systems and HSPs. In the ACT group, a major group of differentially expressed proteins ($n = 7$) were those involved in cellular defense systems against ROS or free radicals. PRDX3, PRDX6, SOD, and glutathione-*S*-transferase-μ2 were upregulated. Consistently, HSPs, including HSP B6 and αβ-crystallin, which also protect cells against oxidative stress, were upregulated.

An enhancement of antioxidant defense systems was observed in the SED group as well, although to a lower extent. Three protein spots corresponding to SOD and HSP B6 (two spots) were upregulated post-NMES.

Other proteins. In the ACT group, three differentially expressed proteins, which were all upregulated, could not be ascribed to a specific functional group: RNA-binding protein regulatory subunit Dj-1, Kelch-related protein 1 (Krp1), and DNAase1.

In the SED group, myoglobin was downregulated, whereas serum albumin and Krp1 were upregulated.

Immunoblot Analysis

To validate the results of the 2-D electrophoresis analysis, comparative immunoblot analysis of some of the most relevant changed proteins was carried out. Comparative analysis of immunoreactive bands was performed for ATP synthase, NADH-ubiquinone oxidoreductase, ubiquinol cytochrome *c* reductase, β-enolase, tubulin, SOD1, PRDX3, and αβ-crystallin in the ACT group (Fig. 9) and acyl CoA, pyruvate dehydrogenase, isocitrate dehydrogenase, ubiquinol cytochrome *c* reductase, lactate dehydrogenase, triosephosphate isomerase, β-enolase, creatine kinase, SOD1, and myoglobin in the SED group (Fig. 10). The immunoblot analysis confirmed the changes in the expression of all proteins except for β-enolase. The latter inconsistency is conceivable. In fact, being that β-enolase separated in 2-D maps in very many spots, the significantly different expression of a single spot cannot ensure a correct determination. Indeed, a major reason to perform immunoblot analysis is to ensure that when a protein is separated in more than one spot the spot that is found to be differentially expressed is representative of the protein as a whole.

DISCUSSION

The goal of the this study was to provide a comprehensive picture of skeletal muscle phenotype adaptations after a typical NMES training program through a combination of both in vivo and in vitro analyses. The proteomic approach has been applied only in one instance to study interval-exercise training-induced adaptations in humans (44) and never to NMES. The proteomic approach enabled us to compare the expression of several hundred proteins (~500) after multiple sessions of NMES. NMES induces atypical adaptations of the muscle phenotype that are characteristic of both resistance (i.e., strength gains) and endurance (i.e., fast-to-slow conversion) training.

In Vivo Adaptations

Neuromuscular tests performed before and after the training program confirmed that NMES is an efficient modality to

Table 1. *Differentially expressed proteins in the SED group pre-NMES versus the ACT group pre-NMES*

Spot Number in Map	Protein Name	Swiss-Prot Accession Number	Theoretical Isoelectric Point Using Expasy Tool	Theoretical Molecular Mass Using Expasy Tool, Da	Ratio
		Myofibrillar proteins			
1	Slow skeletal myosin regulatory light chain, 2s	P10916	4.62	18,789	−1.7
2	Fast skeletal myosin regulatory light chain, 2f	Q96A32	4.91	19,015	2.68
3	Troponin T, fast skeletal muscle	P45378	5.71	31,825	2.48
4	Tropomyosin-α1	P09493	4.69	32,708	4.23
		Glycolytic metabolism			
5	Phosphofructokinase	P08237	8.23	85,182	6.23
6	Triosephosphate isomerase 1	P60174	5.65	31,057	1.86
7	Triosephosphate isomerase 1	P60174	5.65	31,057	3.48
8	Triosephosphate isomerase 1	P60174	5.65	31,057	3.07
9	Glyceraldehyde-3-phosphate dehydrogenase	P04406	8.26	36,202	2.46
10	β-Enolase	P13929	7.59	47,244	4.05
11	Glycogen phosphorylase	P11217	6.57	97,560	3.53
12	Glycogen phosphorylase	P11217	6.57	97,560	5.51
		Oxidative metabolism			
13	Ubiquinol cytochrome *c* reductase complex core protein I, mitochondrial (precursor)	P31930	5.94	53,270	−1.23
14	NADH-ubiquinone oxidoreductase 30-kDa subunit, mitochondrial (precursor)	O75489	5.76	30,242	−1.67
15	Acyl CoA dehydrogenase very-long-chain isoform 1 precursor	P49748	8.92	70,745	−1.94
		Creatine kinase			
16	Creatine kinase	P07310	6.77	43,268	5.76
		Antioxidant defense systems			
17	Carbonic anhydrase III	P07451	6.86	29,557	1.91
18	Carbonic anhydrase III	P07451	6.86	29,557	2.62
		Other proteins			
19	Fatty acid-binding protein	P05413	6.29	14,858	2.83
20	Serum albumin precursor	P02768	5.91	71,176	2.56
21	Myoglobin	P02144	7.29	17,099	1.66
22	Myoglobin	P02144	7.29	17,099	3.35
23	DNAase1	P24855	4.71	31,434	6.07

SED, sedentary; ACT, active; NMES, neuromuscular electrical stimulation.

increase voluntary strength. In agreement with our previous study (36), an average increase of ~30% in MVC force of the knee extensor muscles was observed after 8 wk of NMES training. It is noteworthy that the strength gains can be ascribed, at least partially, to adaptations occurring within the central nervous system. Indeed, neural activation was higher after NMES, which is consistent with our previous reports (35, 36). The occurrence of neural adaptations is related to the fact that NMES does not actually bypass the nervous system. Indeed, NMES activates both intramuscular nerve branches and cutaneous receptors, thus generating force directly by the activation of motor axons (48) and indirectly by reflex recruitment of spinal motoneurons (21). Moreover, activation of various brain areas has been observed during a single bout of NMES performed on the knee extensor muscles (87).

In Vitro Adaptations

NMES and MHC distribution. Although several studies have reported lower MHC-2A and higher MHC-1 contents in young active humans compared with our results (5, 45, 77, 81), the MHC profile of the ACT group at baseline was consistent with that previously reported by our laboratory (11, 24). The very high MHC-2X content (i.e., ranging from 34% to 58%) observed in all the four subjects of the SED group likely reflected their physical training status since similar MHC distribution has been reported in SED subjects (40, 74).

One of the key findings of our study was the shift toward a slower phenotype after NMES regardless of the training status. Whereas a MHC isoform shift in the direction of MHX-2X > MHC-2A has been frequently observed after voluntary resistance strength training (5, 46, 98), the very large shift toward MHC-1, especially in the SED group, was rather unexpected. Indeed, a bidirectional transformation (MHC-1 > MHC-2A < MHC-2X) has been mostly reported after training (31, 61) and also after a 6-wk NMES program (77). Nevertheless, these latter authors (77) have failed to observe muscle hypertrophy and an improvement in functional capacity of the knee extensor muscles, contrary to the considerable increases in strength and single-fiber CSA induced by our NMES protocol. To our knowledge, an increase in MHC-1 content has only been observed after low-frequency (i.e., 15 Hz), high-volume (i.e., 4 h/day, 7 days/wk) NMES (74) or, at a lower extent, after intensive marathon training (95). It appears, therefore, that both high- and low-frequency NMES can increase MHC-1 content. The atypical adaptations we observed could be likely accounted for by the motor unit recruitment during NMES that

Table 2. *Differentially expressed proteins in the ACT group post-NMES versus pre-NMES*

Spot Number in Map	Protein Name	Swiss-Prot Accession Number	Theoretical Isoelectric Point Using Expasy Tool	Theoretical Molecular Mass Using Expasy Tool, Da	Ratio
		Myofibrillar proteins			
24	α-Cardiac actin	P68032	5.31	42,019	1.56
25	Tubulin-β2 chain	P07437	4.83	49,671	1.92
26	Tubulin-β2 chain	P07437	4.83	49,671	2.11
27	α-Skeletal actin	P68133	5.33	42,051	2.63
28	Slow skeletal myosin light chain, 1s	P14649	5.56	22,764	3.20
29	Desmin	P17661	4.99	53,536	2.65
30	Cofilin 2	Q9Y281	7.66	18,839	4.90
		Glycolytic metabolism			
31	β-Enolase	P13929	7.59	47,244	2.48
		Oxidative metabolism			
32	ATP synthase	P06576	4.95	48,083	2.90
14	NADH-ubiquinone oxidoreductase 30-kDa subunit, mitochondrial (precursor)	O75489	5.76	30,242	3.47
13	Ubiquinol cytochrome *c* reductase complex core protein I, mitochondrial (precursor)	P31930	5.94	53,270	2.33
33	Enoyl CoA hydratase, short chain, 1, mitochondrial	P30084	5.95	31,387	3.37
		Antioxidant defense systems and heat shock proteins			
34	Heat shock protein B6	O14558	5.95	17,182	2.83
35	Heat shock protein B6	O14558	5.95	17,182	3.22
36	αβ-Crystallin	P02511	6.76	20,146	1.26
37	Peroxiredoxin 6	P30041	6.0	25,133	1.35
38	Peroxiredoxin 3	P30041	7.67	28,017	2.20
39	Cu/Zn SOD	P00441	5.86	16,096	1.87
40	Glutathione-*S*-transferase-μ2	P28161	6.58	25,745	4.61
		Other proteins			
41	RNA-binding protein regulatory subunit Dj-1	O14805	6.06	19,891	2.41
42	Kelch-related protein 1	O60662	5.14	68,037	3.20
23	DNAase1	P24855	4.71	31,434	2.60

does not strictly follow the well-described Henneman's size principle of voluntary contractions (42). Indeed, NMES allows the recruitment of both slow and fast fibers even at relatively low force levels (random spatial recruitment) (37, 53), knowing that recruitment according to size principle is also possible with the use of wide-pulse (1 ms), high-frequency (50–100 Hz) NMES (i.e., reflex recruitment with central torque development) (21). In addition, NMES induces continuous contractile activity of the same fibers (superficial and spatially fixed recruitment) that inevitably results in early and exaggerated muscle fatigue (for a review, see Ref. 63). On that basis, one could assume that the continuous activation of the same population of muscle fibers, especially of the most fatiguable, fast ones, could explain why a shift toward a slower phenotype occurred. However, further carefully controlled studies are needed to provide additional insights into the role of motor unit recruitment pattern in the magnitude of muscular adaptations.

NMES, muscle mass, and the myofibrillar protein pattern. The gains in maximal voluntary strength were also related to changes at the muscle level since we observed a significant muscle hypertrophy of both type 1 (+12%) and type 2A (+23%) muscle fibers. Using ultrasonography measurements, we (36) have previously reported an increase of 6% in quadriceps muscle anatomic CSA, which is lower than the increase of single-fiber CSA observed here. This is in agreement with Aagaard et al. (1), who observed that single-muscle fiber CSA increased more than anatomic muscle CSA after 14 wk of heavy-resistance voluntary strength training. For technical reasons, however, the CSA analysis was limited to four subjects. Indeed, given the small amount of material obtained by needle biopsy and the need to collect a sufficient amount of tissue to perform MHC, and especially proteomic and immunoblot analyses, a very small portion of the biopsy could be devoted to histological analysis. However, the occurrence of muscle hypertrophy after the same NMES training protocol used in this study is supported not only by in vivo analysis (36) but also by a previous single case study (65) and by an ongoing resistance training study performed in our laboratory, in which a highly significant increase in CSA of individually dissected muscle fibers was observed in 14 healthy subjects (G. D'Antona, M. A. Pellegrino, and R. Bottinelli, unpublished observations).

The increase in CSA might not be the only cellular determinant of strength gains after NMES. Specific force has been shown to be higher in hypertrophic fibers of body builders (24) than in control fibers, and variations in specific force have been observed during a competitive season in male cross-country runners after a change in training volume (39). Therefore, an increase in the intrinsic capacity to develop force by muscles fibers might also concur to the strength gain after NMES. A detailed analysis of such phenomenon is required to define a clear picture of the determinants of strength improvements after NMES.

Table 3. *Differentially expressed proteins in the SED group post-NMES versus pre-NMES*

Spot Number in Map	Protein Name	Swiss-Prot Accession Number	Theoretical Isoelectric Point Using Expasy Tool	Theoretical Molecular Mass Using Expasy Tool, Da	Ratio
		Myofibrillar proteins			
43	Troponin T, fast skeletal muscle	P45378	5.71	31,825	−3.05
44	Fast skeletal myosin regulatory light chain, 2f	Q96A32	4.91	19,015	−5.51
56	Fast skeletal myosin alkali light chain, 1f	P05976	4.97	21,189	2.2
46	Fast skeletal myosin alkali light chain, 1f	P05976	4.97	21,189	−1.28
		Glycolytic metabolism			
47	Phosphofructokinase	P08237	8.23	85,182	−3.23
48	L-Lactate dehydrogenase A chain	P00338	8.44	36,950	−3.11
49	Pyruvate kinase 3 isoform 2	P14618	7.60	58,538	−2.14
50	Pyruvate kinase 3 isoform 2	P14618	7.60	58,538	3.28
8	Triosephosphate isomerase 1	P60174	5.65	31,057	−2.1
9	Glyceraldehyde-3-phosphate dehydrogenase	P04406	8.26	36,202	−1.98
10	β-Enolase	P13929	7.59	47,244	−4.06
51	β-Enolase	P13929	7.59	47,244	−2.46
52	β-Enolase	P13929	7.59	47,244	1.93
53	β-Enolase	P13929	7.59	47,244	2.83
54	β-Enolase	P13929	7.59	47,244	4.25
11	Glycogen phosphorylase	P11217	6.57	97,560	−3.27
55	Glycogen phosphorylase	P11217	6.57	97,560	−3.74
56	Glycogen phosphorylase	P11217	6.57	97,560	−3.32
12	Glycogen phosphorylase	P11217	6.57	97,560	−3.06
57	Glycogen phosphorylase	P11217	6.57	97,560	−3.41
		Oxidative metabolism			
58	Acyl CoA dehydrogenase very-long-chain isoform 1 precursor	P49748	8.92	70,745	−3.87
59	Pyruvate dehydrogenase-β	P11177	5.38	93,233	2.96
60	Isocitrate dehydrogenase 2 ($NADP^+$) mitochondrial precursor	P48735	8.88	51,333	4.38
61	Ubiquinol cytochrome *c* reductase complex core protein I, mitochondrial (precursor)	P31930	5.94	53,270	5.95
		Creatine kinase			
16	Creatine kinase	P07310	6.77	43,268	−2.1

In the ACT group, the adaptations in the MLC profile were fully consistent with the fast-to-slow shift in MHC isoform content.

The upregulation of desmin, tubulin-β2, cofilin-2, and both α-cardiac and α-skeletal actin complements the picture of muscle hypertrophy. Desmin connects adjacent myofibrills at the level of the Z disks and the Z disks with the subsarcolemmal cytoskeleton contributing to the longitudinal and especially lateral load-bearing capacity of muscle fibers. Desmin content has been found to increase after resistance training in healthy humans (100) and after chronic low-frequency stimulation (CLFS) in animals (7), likely indicating an improvement in the load-bearing capacity of the cytoskeleton, whereas disuse has been shown to decrease desmin content (18). In addition, a significant negative correlation between desmin content and the percentage of MHC-2X has been recently reported (100), thereby indicating that muscle containing a smaller percentage of MHC-2X may have a greater desmin protein content. This finding is consistent with the low MHC-2X content (i.e., ~5%) observed at the end of the NMES training. Tubulin-β2 is involved in the polymerization of microtubules, which are implied in numerous cellular processes including intracellular transport, positioning of organelles, cell motility, and mitosis. Considering that microtubules participate in the mechanical integration of various organelles in skeletal muscle, the adaptation of tubulin-β2 can be part of an overall adaptation of the cytoskeleton to higher load bearing. Of interest, microtubules are involved in the early hypertrophic responses of the myocardium during pressure overload (89), and patients treated with colchicine, a microtubule polymerization inhibitor by binding to tubulin, develop "colchicine myopathy," which is characterized by muscle weakness (30). An alternative explanation for the upregulation of tubulin-β2 would be the shift toward a slower phenotype, since microtubules are approximately twofold more abundant in type 1 fibers than in type 2 fibers (15). Cofilin-2 is involved in the regulation of the actin-filament dynamics (8, 19). Donoghue et al. (27) reported increased cofilin-2 content after CLFS and suggested that it could be considered as a new biomarker of fast-to-slow conversion. However, a slower phenotype was observed not only in the ACT group but also in the SED group, whereas the cofilin-2 content remained unchanged. Therefore, changes in the cofilin-2 content are unlikely to depend on the same gene program controlling MHC distribution.

Both the α-skeletal and α-cardiac actin, which are the two isoforms of actin expressed in human skeletal muscle fibers (38), were found to be upregulated. Surprisingly, the α-skeletal actin content was unchanged after multiple bouts of voluntary resistance training (100, 101), suggesting that the pattern of motor unit recruitment might be involved in the specific adaptation of the main thin filament. Indeed, besides our present findings, higher actin content has been observed after CLFS of

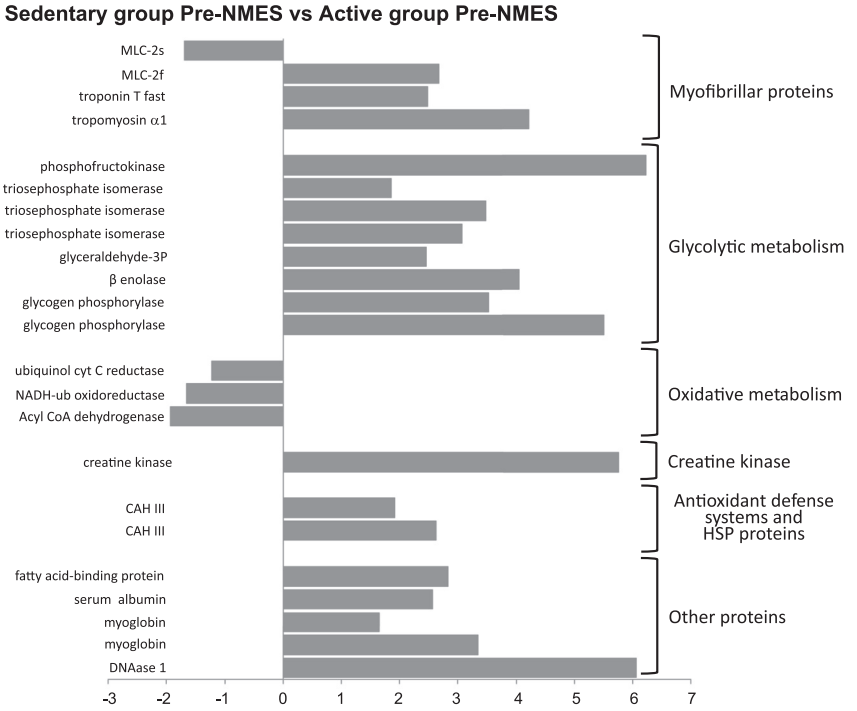

Fig. 5. Histogram of volume ratios of differentially expressed proteins in the SED pre-NMES versus the ACT group pre-NMES. As shown on the *right*, proteins were grouped on the basis of their functional role as follows: myofibrillar proteins, energy production systems (glycolytic metabolism, oxidative metabolism, and creatine kinase), antioxidant defense systems and heat shock proteins (HSPs), and other proteins. The numbers on the *x*-axis indicate the ratio between the average volume of a given protein expressed in the SED group and the average volume of the same protein in the ACT group. Positive numbers (on the *right*) indicate upregulation of a protein in the SED group whereas negative numbers (on the *left*) indicate downregulation. MLC, myosin light chain; CAH III, carbonic anhydrase III.

the rabbit tibialis anterior muscle (27). It should be noted that actin content has been shown to decrease in disuse (18, 85). The upregulation of α-cardiac actin after NMES is intriguing. α-Cardiac actin is the predominant actin isoform in fetal skeletal muscle (75) but is later down-regulated in human skeletal muscle to low levels by birth (49) and accounts for <5% of the striated actin in adult skeletal muscle (96). Interestingly, α-cardiac actin expression in skeletal muscle rescued the lethality of mice lacking α-skeletal actin (73).

Collectively, the changes in desmin, cofilin-2, tubulin-β2 and actin suggest a strengthening of the cytoskeleton of muscle fibers of the ACT group, which can be interpreted as an adaptation to the higher force bearing after NMES. Consistently, Krp1, which promotes the assembly of myofibrils through interactions with nebulin-related anchoring protein and actin (91), was also upregulated.

In the SED group, the adaptations in myofibrillar proteins were not large and could mainly be accounted for by the

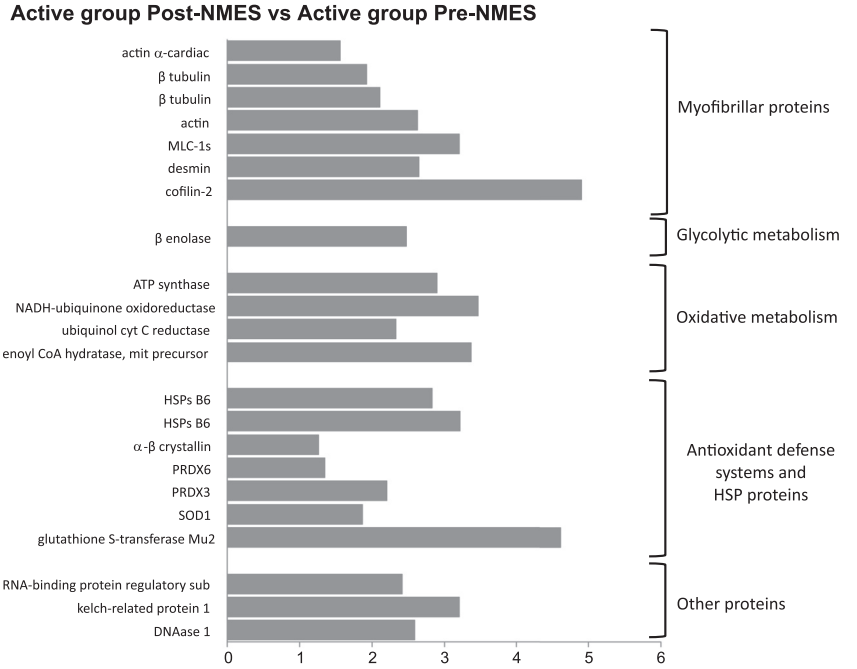

Fig. 6. Histogram of volume ratios of differentially expressed proteins in the ACT group after NMES training. The numbers on the *x*-axis indicate the ratio between the average volume of a given protein expressed after training and the average volume of the same protein before training. Positive numbers (on the *right*) indicate upregulation of a protein after training, whereas negative numbers (on the *left*) indicate downregulation.

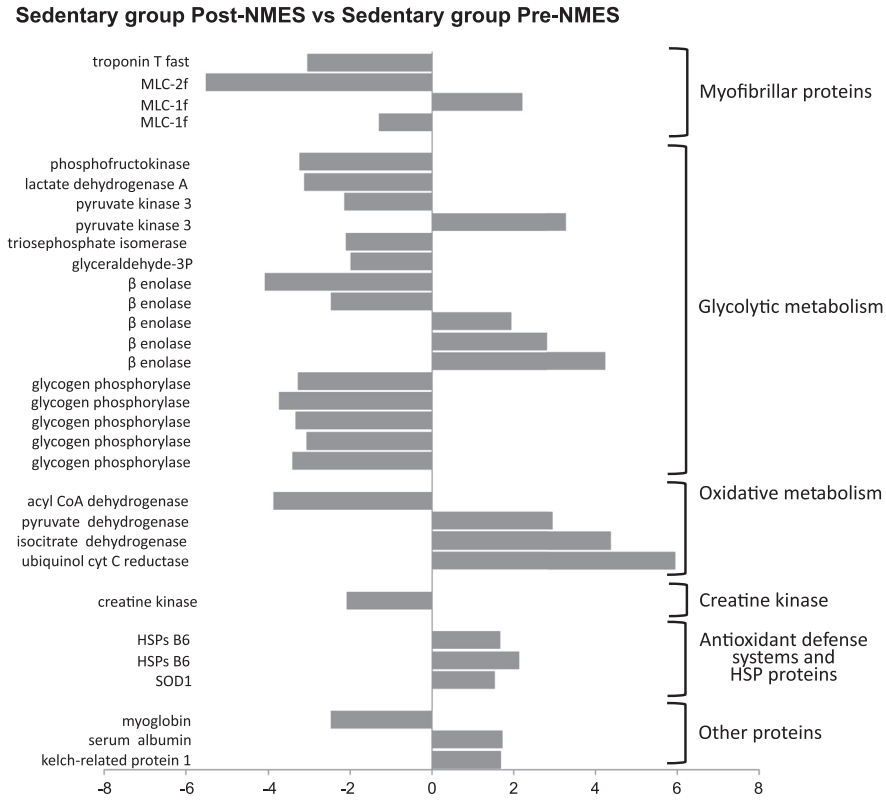

Fig. 7. Histogram of volume ratios of differentially expressed proteins in the SED group after NMES training. The same approach to represent differentially expressed proteins was used as in Fig. 6.

fast-to-slow shift in the MHC profile. In contrast to the ACT group, no significant changes were observed in desmin, tubulin-β2, cofilin-2, actin, or other proteins possibly involved in cytoskeleton remodelling in the SED group. Such differential adaptations between the ACT and SED groups are not easy to explain. It cannot be due to a different content in such proteins at baseline, as the ACT and SED groups showed differences for only MLC, tropomyosin, and troponin isoforms, which were fully consistent with the different MHC profile. A possible clue could come from the trend toward a lower MVC force both pre- and post-NMES by the SED group compared with the ACT group. The adaptations in the cytoskeleton might be triggered or become evident only at higher force levels, i.e., in the ACT group. However, in the absence of a precise determination of force per CSA of the quadriceps muscle, no conclusions can be reached on this issue.

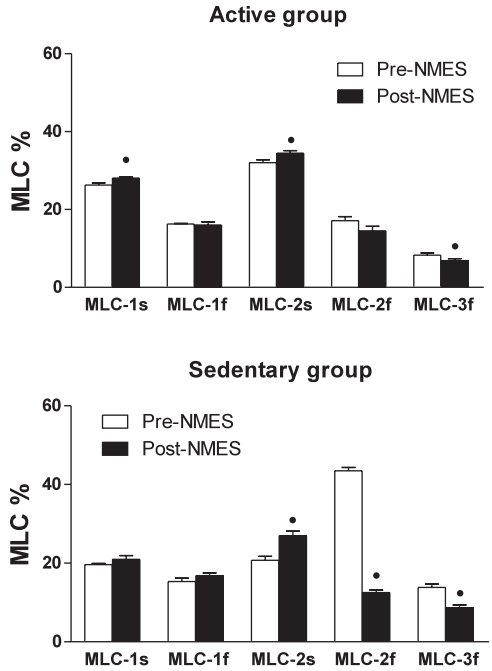

Fig. 8. MLC isoform distribution pre- and post-NMES training for the ACT and SED groups. *Significantly different from pre-NMES ($P < 0.05$).

NMES and energy metabolism. In the ACT group, a general upregulation of oxidative enzymes was observed after training, which is consistent with the fast-to-slow MHC isoform shift and with the increase in mitochondrial volume density that can occur in all fiber types after training (47). β-Enolase, a glycolytic enzyme more abundant in glycolytic, fast fibers (56), has also been shown to be involved in muscle degeneration and regeneration (66). Its upregulation might suggest muscle remodelling after NMES. However, β-enolase was the only protein whose expression was not confirmed by Western blot on one-dimensional gels, likely due to the fact that, being separated in 2-D maps in multiple spots (32, 34), the differential expression of one spot cannot ensure its correct determination. The upregulation of desmin is consistent with and could indeed contribute to a major improvement of cell metabolism. In fact, desmin in not only a load-bearing protein but is also involved in mitochondrial positioning and respiratory function (68). Overall, adaptations of proteins involved in energy metabolism occurring after NMES mimicked those usually observed after endurance training. Interestingly, Perez et al. (77)

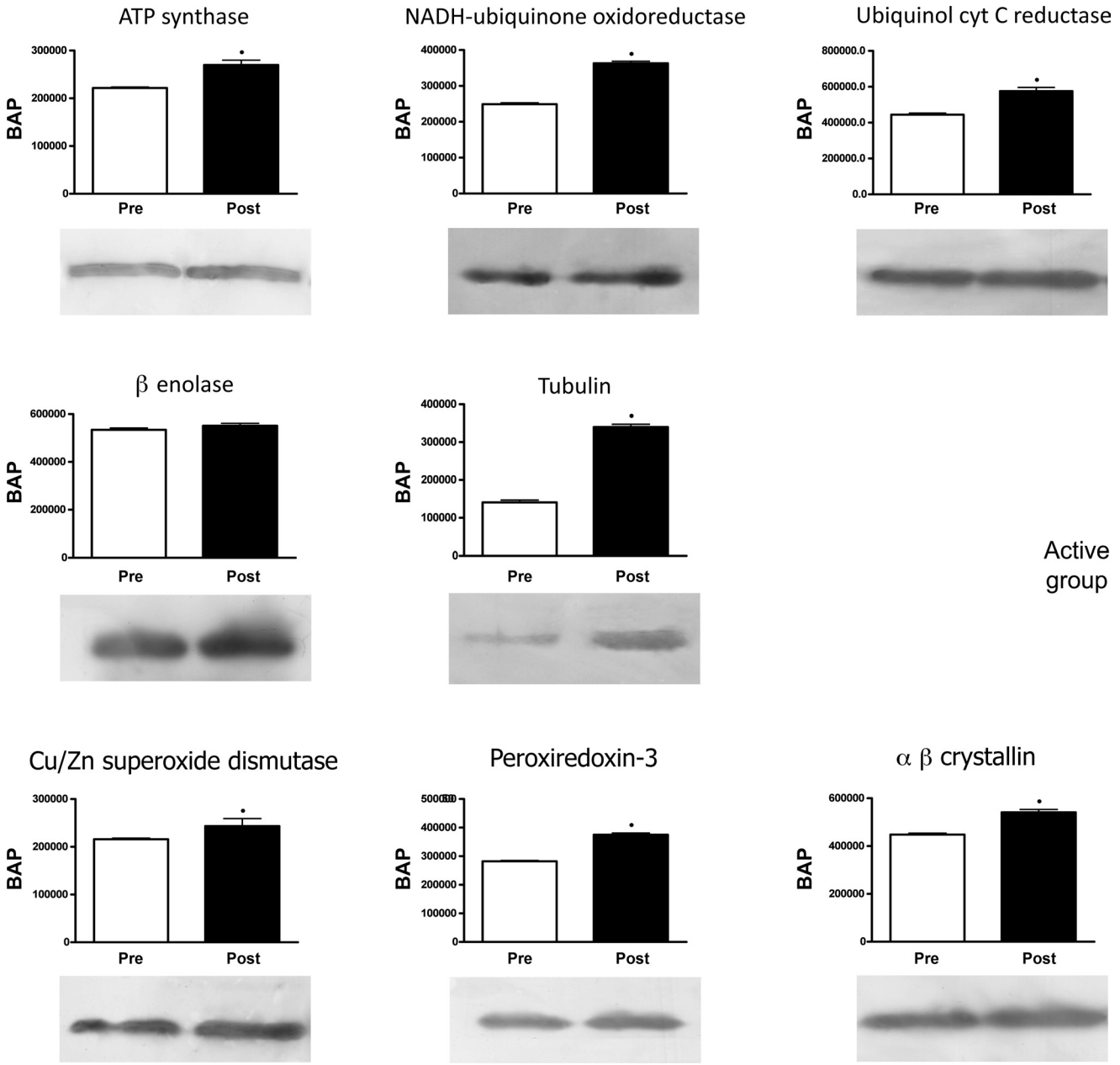

Fig. 9. Confirmation of the proteomic data by Western blot analysis for the ACT group. Shown are immunoreactive bands of ATP synthase, NADH-ubiquinone oxidoreductase, ubiquinol cytochrome *c* reductase, β-enolase, tubulin, SOD1, PRDX3, and αβ-crystallin pre- and post-NMES. *Significantly different from pre-NMES ($P < 0.05$).

reported a higher succinic dehydrogenase activity and an increase in the number of capillaries after a 6-wk NMES training program, whereas both citrate synthase and phosphofructokinase activities were unchanged after 4 wk of NMES (57). As a consequence, it appears that metabolic adaptations occurred concomitantly with changes in muscle mass and architecture (36), i.e., after long-term (i.e., >4 wk) NMES application. Taken together, the adaptations in energy metabolism could be related to the peculiar motor unit recruitment associated with NMES (see above) that imposes an exaggerated metabolic demand (97) and thus hastens the onset of muscle fatigue, mainly because of the repeated contractile activity within the same muscle fibers (63).

In the SED group, the upregulation of oxidative enzymes and the downregulation of glycolytic enzymes and creatine kinase are highly consistent with the fast-to-slow MHC isoform shift as slow fibers mostly have an oxidative metabolism and type 2X fibers mostly have a glycolytic metabolism. In addition, creatine kinase muscle fiber content is known to increase in the order of slow oxidative > fast oxidative glycolytic > fast glycolytic fibers (90). Serum albumin, which is the most abundant protein in human blood plasma, likely comes from blood and small vessels present in the biopsy material. Its upregulation might just be a consequence of the exercise-induced increase in blood vessels (28). Besides its widely recognized short-term O_2 reservoir function, myoglobin

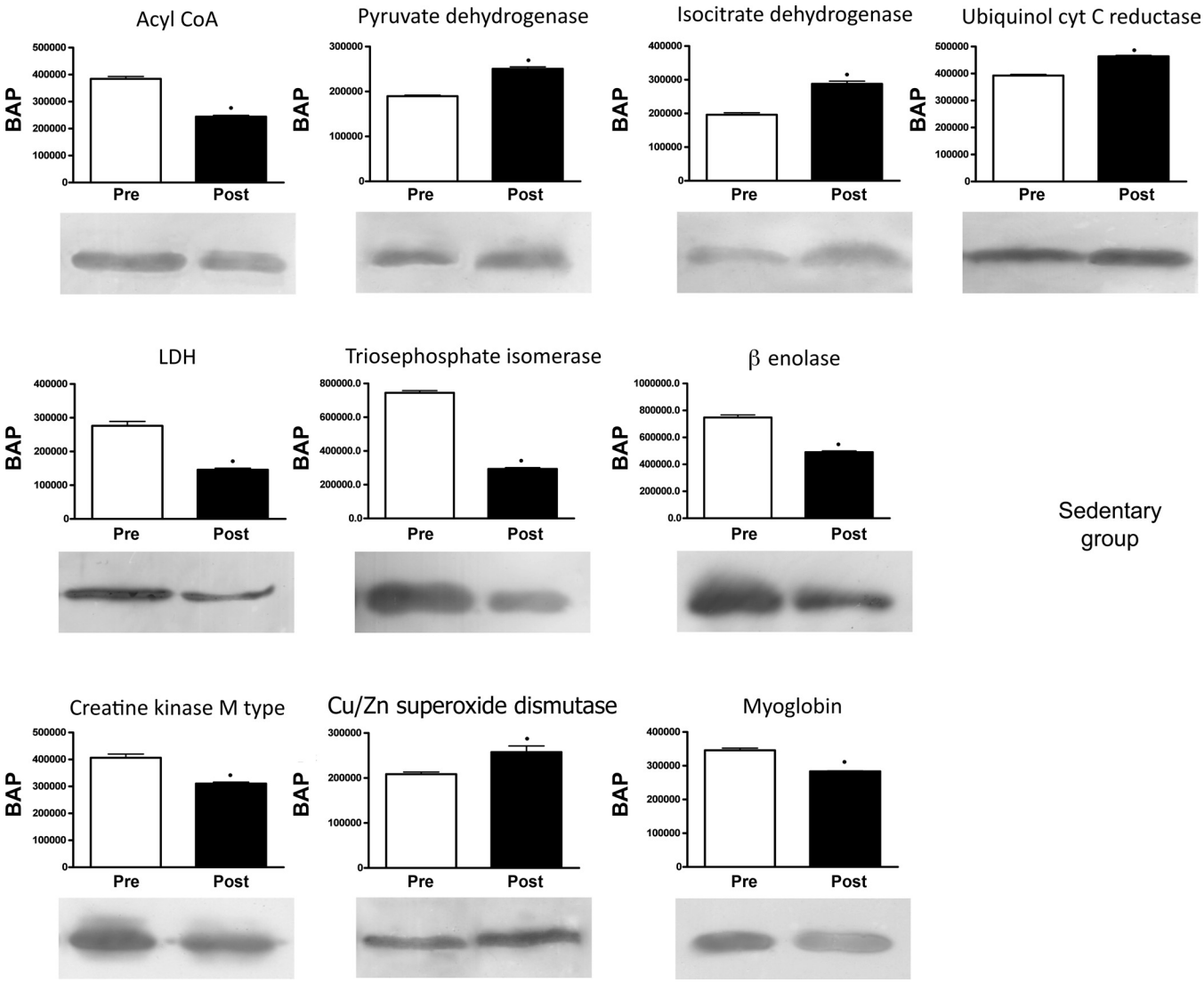

Fig. 10. Confirmation of the proteomic data by Western blot analysis for the SED group. Shown are immunoreactive bands of acyl CoA, pyruvate dehydrogenase, isocitrate dehydrogenase, ubiquinol cytochrome *c* reductase, lactate dehydrogenase (LDH), triosephosphate isomerase, β-enolase, creatine kinase, SOD1, and myoglobin pre- and post-NMES. *Significantly different from pre-NMES ($P < 0.05$).

plays a role in energy metabolism by directly stimulating oxidative phosphorylation and by linking blood O_2 supply to mitochondria, facilitating O_2 diffusion within the cell (67). As type 2A and type 1 fibers have higher myoglobin content than 2X fibers (99), the lower content in myoglobin after NMES in the SED group, confirmed by immunoblot analysis (see Fig. 10), is puzzling. Interestingly, the myoglobin content was unexpectedly higher in the SED group pre-NMES compared with the ACT group pre-NMES. The lower myoglobin content is the only adaptation not consistent with an enhancement of oxidative metabolism.

The different adaptation of the ACT group (no change) versus the SED group (decrease of most enzymes) with respect to glycolytic enzymes likely depends on the starting phenotype of the two groups (Fig. 5). Before NMES, the SED group had a much faster MHC profile and a much higher content in glycolytic enzymes than the ACT group and went through a much larger fast-to-slow shift in MHC isoform content than the ACT group. Given that hypoactive patients are characterized by a fast and glycolytic phenotype, NMES appears particularly suited to induce a shift toward a slower phenotype and a more oxidative metabolism, which would counteract the increased fatiguability.

NMES and oxidative stress. For both groups, HSPs and proteins involved in antioxidant defense systems were mostly upregulated, thereby indicating an improvement of cellular defense systems after multiple bouts of NMES. From the pioneering work of Dillard et al. (26), it is widely accepted that physical exercise results in free radical-mediated damage to tissues. Numerous studies have reported muscle antioxidant adaptation to chronic exercise training (for reviews, see Refs. 50, 51, 52, and 80). Among the antioxidant enzymes in skeletal muscle, SOD activity has consistently been shown to increase with exercise training (23, 43). PRDX, discovered in 1988 (59), is a novel peroxidase capable of reducing both hydroperoxides and peroxynitrate with the use of electrons provided by a physiological thiol, like thioredoxin. Mammalian cells usually express six isoforms of PRDX (PRDX1–6), which are

distributed differentially within the cell: PRDX1, PRDX2, and PRDX6 are found in the cytosol, PRDX3 is located in the mitochondrion, PRDX4 is located in the extracellular space, and PRDX5 is located in both mitochondria and peroxisomes (84). We found an upregulation of PRDX3, and PRX6 after NMES, thereby indicating that adaptations enhancing defenses against oxidative stress occurred within both the cytosol and mitochondrion. Interestingly, a decrease in the expression of PRDX6, coupled to the downregulation of other proteins involved in antioxidant defenses systems, was observed in disuse (18), a condition in which defenses against oxidative stress are supposed to be impaired. While the Dj-1 functional role is still unclear, it has been recently suggested that it could be an atypical peroxiredoxin-like peroxidase participating in antioxidant defense against ROS (6).

Upregulation of HSPs, including HSP B6 [previously named HSP20 (55)] and αβ-crystallin, has been widely observed after chronic voluntary exercise (69). Considering that both small HSPs and αβ-crystallin are also involved in the stabilization of actin filaments and in Z-disk structure remodeling (29, 70, 76), their upregulation is also consistent with the higher content of both desmin and α-skeletal actin and could reflect a protection of the cytoskeleton and contractile machinery. Given that oxidative stress might be directly or indirectly involved in the pathogenesis of various diseases (71), one could suggest that NMES might be an effective modality for enhancing the activity of antioxidant enzymes and counteracting muscle wasting.

Interestingly, the enhancement of antioxidant defense systems and HSPs was much more pronounced in the ACT group than in the SED group. Such a differential response of the two groups was not due to a different expression of antioxidant defense systems pre-NMES. We only observed a higher content of carbonic anhydrase III in the SED group, which is surprising because carbonic anhydrase III content is known to be higher in slow muscle fibers than in fast muscle fibers (102). However, the slower baseline phenotype of the ACT group is likely involved in such phenomenon, as the enhancement of the exercise-induced increase in SOD activity in muscle fibers is greatest in skeletal muscles composed of highly oxidative fibers (e.g., type 1 and type 2A) (23).

As exercise increases the production of ROS, the observed adaptations could be an attempt to maintain the balance between ROS production and removal during exercise, which, in turn, play multiple regulatory roles (80, 83). It is well known that low basal levels of ROS are required for normal force production, small increases in ROS enhance muscle performance, and small decreases or large increases in ROS depress muscle performance. In addition, high levels of ROS can determine muscle damage. Interestingly, growing evidence is emerging illustrating the potential damaging effect of electrically induced isometric contractions in humans. Indeed, three studies (2, 3, 54) have recently reported a significant increased muscle soreness and creatine kinase activity (i.e., from ~10- to 30-fold) resulting from NMES of the quadriceps muscle. Mackey et al. (62) also showed that a NMES session performed on the human gastrocnemius muscles led to macrophage infiltration, z-line disruption, and slightly modified desmin staining, therefore providing direct evidence of fiber alterations.

The differential adaptations of the antioxidant defense systems of the ACT and SED groups to NMES could, therefore, contribute to the variations in muscle performance and muscle adaptations between the two groups after NMES.

Conclusions

In the present study, we demonstrated that NMES training is an efficient modality for increasing muscle mass, maximal voluntary strength, neural drive, and oxidative metabolism as well as for improving antioxidant defense systems in healthy young humans. The atypical adaptations of the muscle phenotype by NMES are characteristic of both resistance (i.e., strength gains) and endurance (i.e., fast-to-slow and glycolytic-to-oxidative conversion) training and can be mainly ascribed to the specific motor unit recruitment pattern, i.e., nonselective, continuous, and synchronous. Considering that disuse atrophy is characterized by loss of muscle mass and strength, by a faster and more glycolytic phenotype, and by an increase in fatiguability, the adaptations observed here on healthy muscles would even be larger for immobilized/disused muscles. In agreement with a recent systematic review of randomized controlled trials (10), NMES appears, therefore, particularly suited to counteract disuse atrophy in hypoactive patients.

ACKNOWLEDGMENTS

Present address of J. Gondin: Centre de Résonance Magnétique Biologique et Médicale (CRMBM), UMR CNRS 6612, Faculté de Médecine, Université de la Méditerranée, 27 Bd. Jean Moulin, 13005, Marseille, France (e-mail: julien.gondin@univmed.fr).

The authors thank CEINGE Advanced Biotecnologies S.C.A.R.L. Center (Naples, Italy) for help in protein identification by MALDI-TOF analysis.

GRANTS

This work was supported by an Italian Space Agency grant (Project "Osteoporosis and Muscle Atrophy") and by MYOAGE Grant HEALTH-F2-2009-223576 ("Understanding and combating age-related muscle weakness") (to R. Bottinelli). During the project, J. Gondin worked at the Department of Physiology, University of Pavia (Pavia, Italy) and was supported by a research fellowship from R. Bottinelli's grants.

DISCLOSURES

No conflicts of interest, financial or otherwise, are declared by the author(s).

REFERENCES

1. **Aagaard P, Andersen JL, Dyhre-Poulsen P, Leffers AM, Wagner A, Magnusson SP, Halkjaer-Kristensen J, Simonsen EB.** A mechanism for increased contractile strength of human pennate muscle in response to strength training: changes in muscle architecture. *J Physiol* 534: 613–623, 2001.
2. **Aldayel A, Jubeau M, McGuigan M, Nosaka K.** Comparison between alternating and pulsed current electrical muscle stimulation for muscle and systemic acute responses. *J Appl Physiol* 109: 735–744, 2010.
3. **Aldayel A, Jubeau M, McGuigan MR, Nosaka K.** Less indication of muscle damage in the second than initial electrical muscle stimulation bout consisting of isometric contractions of the knee extensors. *Eur J Appl Physiol* 108: 709–717, 2010.
4. **Allen GM, Gandevia SC, McKenzie DK.** Reliability of measurements of muscle strength and voluntary activation using twitch interpolation. *Muscle Nerve* 18: 593–600, 1995.
5. **Andersen JL, Aagaard P.** Myosin heavy chain IIX overshoot in human skeletal muscle. *Muscle Nerve* 23: 1095–1104, 2000.
6. **Andres-Mateos E, Perier C, Zhang L, Blanchard-Fillion B, Greco TM, Thomas B, Ko HS, Sasaki M, Ischiropoulos H, Przedborski S, Dawson TM, Dawson VL.** DJ-1 gene deletion reveals that DJ-1 is an atypical peroxiredoxin-like peroxidase. *Proc Natl Acad Sci USA* 104: 14807–14812, 2007.
7. **Baldi JC, Reiser PJ.** Intermediate filament proteins increase during chronic stimulation of skeletal muscle. *J Muscle Res Cell Motil* 16: 587–594, 1995.

8. **Bamburg JR, McGough A, Ono S.** Putting a new twist on actin: ADF/cofilins modulate actin dynamics. *Trends Cell Biol* 9: 364–370, 1999.
9. **Bamman MM, Petrella JK, Kim JS, Mayhew DL, Cross JM.** Cluster analysis tests the importance of myogenic gene expression during myofiber hypertrophy in humans. *J Appl Physiol* 102: 2232–2239, 2007.
10. **Bax L, Staes F, Verhagen A.** Does neuromuscular electrical stimulation strengthen the quadriceps femoris? A systematic review of randomised controlled trials. *Sports Med* 35: 191–212, 2005.
11. **Borina E, Pellegrino MA, D'Antona G, Bottinelli R.** Myosin and actin content of human skeletal muscle fibers following 35 days bed rest. *Scand J Med Sci Sports* 20: 65–73, 2010.
12. **Bottinelli R, Canepari M, Pellegrino MA, Reggiani C.** Force-velocity properties of human skeletal muscle fibres: myosin heavy chain isoform and temperature dependence. *J Physiol* 495: 573–586, 1996.
13. **Bottinelli R, Reggiani C.** Human skeletal muscle fibres: molecular and functional diversity. *Prog Biophys Mol Biol* 73: 195–262, 2000.
14. **Bottinelli R, Schiaffino S, Reggiani C.** Force-velocity relations and myosin heavy chain isoform compositions of skinned fibres from rat skeletal muscle. *J Physiol* 437: 655–672, 1991.
15. **Boudriau S, Vincent M, Cote CH, Rogers PA.** Cytoskeletal structure of skeletal muscle: identification of an intricate exosarcomeric microtubule lattice in slow- and fast-twitch muscle fibers. *J Histochem Cytochem* 41: 1013–1021, 1993.
16. **Bourjeily-Habr G, Rochester CL, Palermo F, Snyder P, Mohsenin V.** Randomised controlled trial of transcutaneous electrical muscle stimulation of the lower extremities in patients with chronic obstructive pulmonary disease. *Thorax* 57: 1045–1049, 2002.
17. **Brocca L, D'Antona G, Bachi A, Pellegrino MA.** Amino acid supplements improve native antioxidant enzyme expression in the skeletal muscle of diabetic mice. *Am J Cardiol* 101: 57E–62E, 2008.
18. **Brocca L, Pellegrino MA, Desaphy JF, Pierno S, Camerino DC, Bottinelli R.** Is oxidative stress a cause or consequence of disuse muscle atrophy in mice? A proteomic approach in hindlimb-unloaded mice. *Exp Physiol* 95: 331–350, 2010.
19. **Chhabra D, dos Remedios CG.** Cofilin, actin and their complex observed in vivo using fluorescence resonance energy transfer. *Biophys J* 89: 1902–1908, 2005.
20. **Coffey VG, Hawley JA.** The molecular bases of training adaptation. *Sports Med* 37: 737–763, 2007.
21. **Collins DF, Burke D, Gandevia SC.** Sustained contractions produced by plateau-like behaviour in human motoneurones. *J Physiol* 538: 289–301, 2002.
22. **Crevenna R, Marosi C, Schmidinger M, Fialka-Moser V.** Neuromuscular electrical stimulation for a patient with metastatic lung cancer–a case report. *Support Care Cancer* 14: 970–973, 2006.
23. **Criswell D, Powers S, Dodd S, Lawler J, Edwards W, Renshler K, Grinton S.** High intensity training-induced changes in skeletal muscle antioxidant enzyme activity. *Med Sci Sports Exerc* 25: 1135–1140, 1993.
24. **D'Antona G, Lanfranconi F, Pellegrino MA, Brocca L, Adami R, Rossi R, Moro G, Miotti D, Canepari M, Bottinelli R.** Skeletal muscle hypertrophy and structure and function of skeletal muscle fibres in male body builders. *J Physiol* 570: 611–627, 2006.
25. **D'Antona G, Pellegrino MA, Adami R, Rossi R, Carlizzi CN, Canepari M, Saltin B, Bottinelli R.** The effect of ageing and immobilization on structure and function of human skeletal muscle fibres. *J Physiol* 552: 499–511, 2003.
26. **Dillard CJ, Litov RE, Savin WM, Dumelin EE, Tappel AL.** Effects of exercise, vitamin E, and ozone on pulmonary function and lipid peroxidation. *J Appl Physiol* 45: 927–932, 1978.
27. **Donoghue P, Doran P, Wynne K, Pedersen K, Dunn MJ, Ohlendieck K.** Proteomic profiling of chronic low-frequency stimulated fast muscle. *Proteomics* 7: 3417–3430, 2007.
28. **Egginton S.** Invited review: activity-induced angiogenesis. *Pflügers Arch* 457: 963–977, 2009.
29. **Feasson L, Stockholm D, Freyssenet D, Richard I, Duguez S, Beckmann JS, Denis C.** Molecular adaptations of neuromuscular disease-associated proteins in response to eccentric exercise in human skeletal muscle. *J Physiol* 543: 297–306, 2002.
30. **Fernandez C, Figarella-Branger D, Alla P, Harle JR, Pellissier JF.** Colchicine myopathy: a vacuolar myopathy with selective type I muscle fiber involvement. An immunohistochemical and electron microscopic study of two cases. *Acta Neuropathol* 103: 100–106, 2002.
31. **Fluck M, Hoppeler H.** Molecular basis of skeletal muscle plasticity–from gene to form and function. *Rev Physiol Biochem Pharmacol* 146: 159–216, 2003.
32. **Gannon J, Staunton L, O'Connell K, Doran P, Ohlendieck K.** Phosphoproteomic analysis of aged skeletal muscle. *Int J Mol Med* 22: 33–42, 2008.
33. **Gauthier JM, Theriault R, Theriault G, Gelinas Y, Simoneau JA.** Electrical stimulation-induced changes in skeletal muscle enzymes of men and women. *Med Sci Sports Exerc* 24: 1252–1256, 1992.
34. **Gelfi C, Vigano A, Ripamonti M, Pontoglio A, Begum S, Pellegrino MA, Grassi B, Bottinelli R, Wait R, Cerretelli P.** The human muscle proteome in aging. *J Proteome Res* 5: 1344–1353, 2006.
35. **Gondin J, Duclay J, Martin A.** Soleus- and gastrocnemii-evoked V-wave responses increase after neuromuscular electrical stimulation training. *J Neurophysiol* 95: 3328–3335, 2006.
36. **Gondin J, Guette M, Ballay Y, Martin A.** Electromyostimulation training effects on neural drive and muscle architecture. *Med Sci Sports Exerc* 37: 1291–1299, 2005.
37. **Gregory CM, Bickel CS.** Recruitment patterns in human skeletal muscle during electrical stimulation. *Phys Ther* 85: 358–364, 2005.
38. **Gunning P, Ponte P, Okayama H, Engel J, Blau H, Kedes L.** Isolation and characterization of full-length cDNA clones for human α-, β-, and γ-actin mRNAs: skeletal but not cytoplasmic actins have an amino-terminal cysteine that is subsequently removed. *Mol Cell Biol* 3: 787–795, 1983.
39. **Harber M, Trappe S.** Single muscle fiber contractile properties of young competitive distance runners. *J Appl Physiol* 105: 629–636, 2008.
40. **Harber MP, Fry AC, Rubin MR, Smith JC, Weiss LW.** Skeletal muscle and hormonal adaptations to circuit weight training in untrained men. *Scand J Med Sci Sports* 14: 176–185, 2004.
41. **Harridge SD, Bottinelli R, Canepari M, Pellegrino MA, Reggiani C, Esbjornsson M, Saltin B.** Whole-muscle and single-fibre contractile properties and myosin heavy chain isoforms in humans. *Pflügers Arch* 432: 913–920, 1996.
42. **Henneman E, Somjen G, Carpenter DO.** Functional significance of cell size in spinal notoneurons. *J Neurophysiol* 28: 560–580, 1965.
43. **Higuchi M, Cartier LJ, Chen M, Holloszy JO.** Superoxide dismutase and catalase in skeletal muscle: adaptive response to exercise. *J Gerontol* 40: 281–286, 1985.
44. **Holloway KV, O'Gorman M, Woods P, Morton JP, Evans L, Cable NT, Goldspink DF, Burniston JG.** Proteomic investigation of changes in human vastus lateralis muscle in response to interval-exercise training. *Proteomics* 9: 5155–5174, 2009.
45. **Holm L, Reitelseder S, Pedersen TG, Doessing S, Petersen SG, Flyvbjerg A, Andersen JL, Aagaard P, Kjaer M.** Changes in muscle size and MHC composition in response to resistance exercise with heavy and light loading intensity. *J Appl Physiol* 105: 1454–1461, 2008.
46. **Hortobagyi T, Dempsey L, Fraser D, Zheng D, Hamilton G, Lambert J, Dohm L.** Changes in muscle strength, muscle fibre size and myofibrillar gene expression after immobilization and retraining in humans. *J Physiol* 524: 293–304, 2000.
47. **Howald H, Hoppeler H, Claassen H, Mathieu O, Straub R.** Influences of endurance training on the ultrastructural composition of the different muscle fiber types in humans. *Pflügers Arch* 403: 369–376, 1985.
48. **Hultman E, Sjoholm H, Jaderholm-Ek I, Krynicki J.** Evaluation of methods for electrical stimulation of human skeletal muscle in situ. *Pflügers Arch* 398: 139–141, 1983.
49. **Ilkovski B, Clement S, Sewry C, North KN, Cooper ST.** Defining α-skeletal and α-cardiac actin expression in human heart and skeletal muscle explains the absence of cardiac involvement in ACTA1 nemaline myopathy. *Neuromuscul Disord* 15: 829–835, 2005.
50. **Jenkins RR.** Free radical chemistry. Relationship to exercise. *Sports Med* 5: 156–170, 1988.
51. **Ji LL.** Exercise and oxidative stress: role of the cellular antioxidant systems. *Exerc Sport Sci Rev* 23: 135–166, 1995.
52. **Ji LL.** Modulation of skeletal muscle antioxidant defense by exercise: role of redox signaling. *Free Radic Biol Med* 44: 142–152, 2008.
53. **Jubeau M, Gondin J, Martin A, Sartorio A, Maffiuletti NA.** Random motor unit activation by electrostimulation. *Int J Sports Med* 28: 901–904, 2007.
54. **Jubeau M, Sartorio A, Marinone PG, Agosti F, Van Hoecke J, Nosaka K, Maffiuletti NA.** Comparison between voluntary and stimulated contractions of the quadriceps femoris for growth hormone response and muscle damage. *J Appl Physiol* 104: 75–81, 2008.

55. **Kampinga HH, Hageman J, Vos MJ, Kubota H, Tanguay RM, Bruford EA, Cheetham ME, Chen B, Hightower LE.** Guidelines for the nomenclature of the human heat shock proteins. *Cell Stress Chaperones* 14: 105–111, 2009.
56. **Keller A, Demeurie J, Merkulova T, Geraud G, Cywiner-Golenzer C, Lucas M, Chatelet FP.** Fibre-type distribution and subcellular localisation of α and β enolase in mouse striated muscle. *Biol Cell* 92: 527–535, 2000.
57. **Kim CK, Takala TE, Seger J, Karpakka J.** Training effects of electrically induced dynamic contractions in human quadriceps muscle. *Aviat Space Environ Med* 66: 251–255, 1995.
58. **Kim JS, Petrella JK, Cross JM, Bamman MM.** Load-mediated downregulation of myostatin mRNA is not sufficient to promote myofiber hypertrophy in humans: a cluster analysis. *J Appl Physiol* 103: 1488–1495, 2007.
59. **Kim K, Kim IH, Lee KY, Rhee SG, Stadtman ER.** The isolation and purification of a specific "protector" protein which inhibits enzyme inactivation by a thiol/Fe(III)/O_2 mixed-function oxidation system. *J Biol Chem* 263: 4704–4711, 1988.
60. **Lake DA.** Neuromuscular electrical stimulation. An overview and its application in the treatment of sports injuries. *Sports Med* 13: 320–336, 1992.
61. **Liu Y, Schlumberger A, Wirth K, Schmidtbleicher D, Steinacker JM.** Different effects on human skeletal myosin heavy chain isoform expression: strength vs. combination training. *J Appl Physiol* 94: 2282–2288, 2003.
62. **Mackey AL, Bojsen-Moller J, Qvortrup K, Langberg H, Suetta C, Kalliokoski KK, Kjaer M, Magnusson SP.** Evidence of skeletal muscle damage following electrically stimulated isometric muscle contractions in humans. *J Appl Physiol* 105: 1620–1627, 2008.
63. **Maffiuletti NA.** Physiological and methodological considerations for the use of neuromuscular electrical stimulation. *Eur J Appl Physiol* 110: 223–234, 2010.
64. **Maffiuletti NA, Dugnani S, Folz M, Di Pierno E, Mauro F.** Effect of combined electrostimulation and plyometric training on vertical jump height. *Med Sci Sports Exerc* 34: 1638–1644, 2002.
65. **Maffiuletti NA, Zory R, Miotti D, Pellegrino MA, Jubeau M, Bottinelli R.** Neuromuscular adaptations to electrostimulation resistance training. *Am J Phys Med Rehabil* 85: 167–175, 2006.
66. **Merkulova T, Dehaupas M, Nevers MC, Creminon C, Alameddine H, Keller A.** Differential modulation of α, β and γ enolase isoforms in regenerating mouse skeletal muscle. *Eur J Biochem* 267: 3735–3743, 2000.
67. **Merx MW, Flogel U, Stumpe T, Godecke A, Decking UK, Schrader J.** Myoglobin facilitates oxygen diffusion. *FASEB J* 15: 1077–1079, 2001.
68. **Milner DJ, Mavroidis M, Weisleder N, Capetanaki Y.** Desmin cytoskeleton linked to muscle mitochondrial distribution and respiratory function. *J Cell Biol* 150: 1283–1298, 2000.
69. **Morton JP, Kayani AC, McArdle A, Drust B.** The exercise-induced stress response of skeletal muscle, with specific emphasis on humans. *Sports Med* 39: 643–662, 2009.
70. **Mounier N, Arrigo AP.** Actin cytoskeleton and small heat shock proteins: how do they interact? *Cell Stress Chaperones* 7: 167–176, 2002.
71. **Moylan JS, Reid MB.** Oxidative stress, chronic disease, and muscle wasting. *Muscle Nerve* 35: 411–429, 2007.
72. **Neder JA, Sword D, Ward SA, Mackay E, Cochrane LM, Clark CJ.** Home based neuromuscular electrical stimulation as a new rehabilitative strategy for severely disabled patients with chronic obstructive pulmonary disease (COPD). *Thorax* 57: 333–337, 2002.
73. **Nowak KJ, Ravenscroft G, Jackaman C, Filipovska A, Davies SM, Lim EM, Squire SE, Potter AC, Baker E, Clement S, Sewry CA, Fabian V, Crawford K, Lessard JL, Griffiths LM, Papadimitriou JM, Shen Y, Morahan G, Bakker AJ, Davies KE, Laing NG.** Rescue of skeletal muscle α-actin-null mice by cardiac (fetal) α-actin. *J Cell Biol* 185: 903–915, 2009.
74. **Nuhr M, Crevenna R, Gohlsch B, Bittner C, Pleiner J, Wiesinger G, Fialka-Moser V, Quittan M, Pette D.** Functional and biochemical properties of chronically stimulated human skeletal muscle. *Eur J Appl Physiol* 89: 202–208, 2003.
75. **Ordahl CP.** The skeletal and cardiac α-actin genes are coexpressed in early embryonic striated muscle. *Dev Biol* 117: 488–492, 1986.
76. **Paulsen G, Vissing K, Kalhovde JM, Ugelstad I, Bayer ML, Kadi F, Schjerling P, Hallen J, Raastad T.** Maximal eccentric exercise induces a rapid accumulation of small heat shock proteins on myofibrils and a delayed HSP70 response in humans. *Am J Physiol Regul Integr Comp Physiol* 293: R844–R853, 2007.
77. **Perez M, Lucia A, Rivero JL, Serrano AL, Calbet JA, Delgado MA, Chicharro JL.** Effects of transcutaneous short-term electrical stimulation on M. vastus lateralis characteristics of healthy young men. *Pflügers Arch* 443: 866–874, 2002.
78. **Petrella JK, Kim JS, Cross JM, Kosek DJ, Bamman MM.** Efficacy of myonuclear addition may explain differential myofiber growth among resistance-trained young and older men and women. *Am J Physiol Endocrinol Metab* 291: E937–E946, 2006.
79. **Petrella JK, Kim JS, Mayhew DL, Cross JM, Bamman MM.** Potent myofiber hypertrophy during resistance training in humans is associated with satellite cell-mediated myonuclear addition: a cluster analysis. *J Appl Physiol* 104: 1736–1742, 2008.
80. **Powers SK, Jackson MJ.** Exercise-induced oxidative stress: cellular mechanisms and impact on muscle force production. *Physiol Rev* 88: 1243–1276, 2008.
81. **Putman CT, Xu X, Gillies E, MacLean IM, Bell GJ.** Effects of strength, endurance and combined training on myosin heavy chain content and fibre-type distribution in humans. *Eur J Appl Physiol* 92: 376–384, 2004.
82. **Quittan M, Wiesinger GF, Sturm B, Puig S, Mayr W, Sochor A, Paternostro T, Resch KL, Pacher R, Fialka-Moser V.** Improvement of thigh muscles by neuromuscular electrical stimulation in patients with refractory heart failure: a single-blind, randomized, controlled trial. *Am J Phys Med Rehabil* 80: 206–215 and 224, 2001.
83. **Reid MB.** Invited Review: redox modulation of skeletal muscle contraction: what we know and what we don't. *J Appl Physiol* 90: 724–731, 2001.
84. **Rhee SG, Kang SW, Netto LE, Seo MS, Stadtman ER.** A family of novel peroxidases, peroxiredoxins. *Biofactors* 10: 207–209, 1999.
85. **Riley DA, Bain JL, Thompson JL, Fitts RH, Widrick JJ, Trappe SW, Trappe TA, Costill DL.** Thin filament diversity and physiological properties of fast and slow fiber types in astronaut leg muscles. *J Appl Physiol* 92: 817–825, 2002.
86. **Schiaffino S, Reggiani C.** Molecular diversity of myofibrillar proteins: gene regulation and functional significance. *Physiol Rev* 76: 371–423, 1996.
87. **Smith GV, Alon G, Roys SR, Gullapalli RP.** Functional MRI determination of a dose-response relationship to lower extremity neuromuscular electrical stimulation in healthy subjects. *Exp Brain Res* 150: 33–39, 2003.
88. **Spangenburg EE, Booth FW.** Molecular regulation of individual skeletal muscle fibre types. *Acta Physiol Scand* 178: 413–424, 2003.
89. **Takahashi M, Tsutsui H, Tagawa H, Igarashi-Saito K, Imanaka-Yoshida K, Takeshita A.** Microtubules are involved in early hypertrophic responses of myocardium during pressure overload. *Am J Physiol Heart Circ Physiol* 275: H341–H348, 1998.
90. **Takekura H, Yoshioka T.** Determination of metabolic profiles on single muscle fibres of different types. *J Muscle Res Cell Motil* 8: 342–348, 1987.
91. **Taylor A, Obholz K, Linden G, Sadiev S, Klaus S, Carlson KD.** DNA sequence and muscle-specific expression of human sarcosin transcripts. *Mol Cell Biochem* 183: 105–112, 1998.
92. **Theriault R, Boulay MR, Theriault G, Simoneau JA.** Electrical stimulation-induced changes in performance and fiber type proportion of human knee extensor muscles. *Eur J Appl Physiol Occup Physiol* 74: 311–317, 1996.
93. **Theriault R, Theriault G, Simoneau JA.** Human skeletal muscle adaptation in response to chronic low-frequency electrical stimulation. *J Appl Physiol* 77: 1885–1889, 1994.
94. **Toigo M, Boutellier U.** New fundamental resistance exercise determinants of molecular and cellular muscle adaptations. *Eur J Appl Physiol* 97: 643–663, 2006.
95. **Trappe S, Harber M, Creer A, Gallagher P, Slivka D, Minchev K, Whitsett D.** Single muscle fiber adaptations with marathon training. *J Appl Physiol* 101: 721–727, 2006.
96. **Vandekerckhove J, Bugaisky G, Buckingham M.** Simultaneous expression of skeletal muscle and heart actin proteins in various striated muscle tissues and cells. A quantitative determination of the two actin isoforms. *J Biol Chem* 261: 1838–1843, 1986.
97. **Vanderthommen M, Duteil S, Wary C, Raynaud JS, Leroy-Willig A, Crielaard JM, Carlier PG.** A comparison of voluntary and electrically

induced contractions by interleaved ^{1}H- and ^{31}P-NMRS in humans. *J Appl Physiol* 94: 1012–1024, 2003.
98. **Williamson DL, Gallagher PM, Carroll CC, Raue U, Trappe SW.** Reduction in hybrid single muscle fiber proportions with resistance training in humans. *J Appl Physiol* 91: 1955–1961, 2001.
99. **Wittenberg BA, Wittenberg JB.** Transport of oxygen in muscle. *Annu Rev Physiol* 51: 857–878, 1989.
100. **Woolstenhulme MT, Conlee RK, Drummond MJ, Stites AW, Parcell AC.** Temporal response of desmin and dystrophin proteins to progressive resistance exercise in human skeletal muscle. *J Appl Physiol* 100: 1876–1882, 2006.
101. **Woolstenhulme MT, Jutte LS, Drummond MJ, Parcell AC.** Desmin increases with high-intensity concentric contractions in humans. *Muscle Nerve* 31: 20–24, 2005.
102. **Zheng A, Rahkila P, Vuori J, Rasi S, Takala T, Vaananen HK.** Quantification of carbonic anhydrase III and myoglobin in different fiber types of human psoas muscle. *Histochemistry* 97: 77–81, 1992.